DTU Library

Catalytic upgrading of tars generated in a 100 kWth low temperature circulating fluidized bed gasifier for production of liquid bio-fuels in a polygeneration scheme

Eschenbacher, Andreas; Jensen, Peter Arendt; Henriksen, Ulrik Birk; Ahrenfeldt, Jesper; Jensen, Claus Dalsgaard; Li, Chengxin; Enemark-Rasmussen, Kasper; Duus, Jens Øllgaard; Mentzel, Uffe Vie; Jensen, Anker Degn

Published in:
Energy Conversion and Management

Link to article, DOI:
10.1016/j.enconman.2020.112538

Publication date:
2020

Document Version
Peer reviewed version

Citation (APA):
Eschenbacher, A., Jensen, P. A., Henriksen, U. B., Ahrenfeldt, J., Jensen, C. D., Li, C., Enemark-Rasmussen, K., Duus, J. Ø., Mentzel, U. V., & Jensen, A. D. (2020). Catalytic upgrading of tars generated in a 100 kWth low temperature circulating fluidized bed gasifier for production of liquid bio-fuels in a polygeneration scheme. *Energy Conversion and Management*, *207*, Article 112538. https://doi.org/10.1016/j.enconman.2020.112538

Catalytic upgrading of tars generated in a 100 kW_{th} low temperature circulating fluidized bed gasifier for production of liquid bio-fuels in a polygeneration scheme

Andreas Eschenbacher[a], Peter Arendt Jensen[a], Ulrik Birk Henriksen[b], Jesper Ahrenfeldt[b], Claus Dalsgaard Jensen[b], Chengxin Li[c], Kasper Enemark-Rasmussen[c], Jens Øllgaard Duus[c], Uffe Vie Mentzel[d], and Anker Degn Jensen[a]

[a]DTU Chemical Engineering, Technical University of Denmark, Søltofts Plads 229, 2800 Kgs. Lyngby, Denmark

[b]DTU Chemical Engineering, Technical University of Denmark, Frederiksborgvej 399, 4000 Risø, Denmark

[c]DTU, Chemistry, Technical University of Denmark, Kemitorvet Building 207, 2800 Kgs. Lyngby, Denmark

[d]Haldor Topsøe A/S, Haldor Topsøes Allé 1, 2800 Kgs. Lyngby, Denmark

ABSTRACT

Gasification of wheat straw, an agricultural residue with high ash content, was investigated in a low temperature circulating fluidized bed (LT-CFB) gasifier in combination with catalytic tar upgrading as a flexible process to co-produce high quality bio-oil, nutrient rich char, and utilize the producer gas for heat and power production. The change in product distribution and bio-oil quality was studied when conducting the catalytic treatment with HZSM-5/γ-Al_2O_3 and lower-cost γ-Al_2O_3. The fuel properties of the raw and upgraded bio-oils were analyzed by elemental composition, moisture, total acid number, size exclusion chromatography, basic nitrogen content, gas chromatography–mass spectrometry with flame ionization detection (GC–MS/FID), ^{1}H nuclear magnetic resonance (NMR), ^{13}C NMR, and two-dimensional heteronuclear single-quantum correlation (2D HSQC) NMR. The operating temperature of the LT-CFB pyrolysis chamber determined the tar yield and quality in the producer gas. With decrease in pyrolysis temperature from 690 to 570 °C, the tar concentration in the producer gas increased while the higher heating value of the condensed oil phase decreased from ~35 to 30 MJ/kg and the oxygen content, moisture content and acidity of the bio-oil increased. Both HZSM-5/γ-Al_2O_3 and γ-Al_2O_3 were effective catalysts as the tar treatment improved the bio-oil quality in terms of increased heating value and revaporization efficiency, and a reduction in oxygen content, moisture content, total acid number, and basic nitrogen content. Catalytic vapor treatment, e.g. using HZSM-5/γ-Al_2O_3 at 500 °C, decreased the energy content in the condensed bio-oil slightly from ~22% to ~20%. The oil quality improved significantly, as the oxygen content (water-free) and TAN of the bio-oil decreased from 13 wt% O and 34 mg KOH/g to 11 wt% O and 3 mg KOH/g, respectively. The catalytically treated bio-oils are thus better suited for further processing in existing oil refineries.

KEYWORDS
pyrolysis; gasification; wheat straw; bio-fuel; catalysis; polygeneration;

1 INTRODUCTION

The reduction of greenhouse gas emissions and the independence of fossil fuels are central and challenging tasks worldwide. Valuable potential synergies between energy production, food supply, waste disposal etc. should be identified and integrated. The use of biomass instead of fossil fuels for electricity and heat production allows for significant reduction in CO_2 emissions. Biomass can be converted into a controllable and reliable supply of electricity and heat. In addition, biomass can also be used to produce different value-added products such as storable high energy density fuels, chemicals and valuable ashes. Biomass feedstocks often have a high content of essential nutrients that can be efficiently recycled in the form of ash or char for use as fertilizer and soil enhancer [1].

Thermal pyrolysis and gasification can be applied to convert many different biomass feedstocks to a wide range of useful products. The low temperature (LT) circulating fluid bed (CFB) gasification process has been developed by the company Ørsted (former Dong Energy) from Denmark in a collaboration with the Technical University of Denmark (DTU) and Danish Fluid Bed Technology. The gasifier consists of two stages, as shown in **Fig. 1**. The LT-CFB concept was originally developed to use high alkali biomass such as straw. By using relatively low reactor temperatures, the straw can be gasified without agglomeration problems in this gasifier. The generated tar rich gas could then be combusted in a power plant boiler that was not designed for biomass combustion, and thereby an alkali rich biomass can be used for production of electricity and heat [2]. At the first stage, a circulating fluidized bed pyrolysis reactor is operated at ~650 °C. Char and sand are separated in a primary cyclone from the vapor stream, and the char is gasified with air and steam at the second stage in a bubbling fluidized bed reactor operated at about 730 °C. The gasifier is operated auto-thermally by using air as the oxidizing medium. The remaining sand, ash, and gas after char gasification are directed to the pyrolysis reactor, and provides the heat for the biomass pyrolysis. Further downstream separation of char and ash fines is achieved with a secondary cyclone and hot gas filtration. The scalability of the unit has been proven from 100 kW to 500 kW, and 6 MW thermal capacity [3]. Cold gas efficiencies of 87–93% have been achieved in tests with the 500 kW_{th} unit [4]. Gas compositions of 6.9% H_2, 12.3% CO, 17.9% CO_2, and 4.5% CH_4 have been reported when using straw pellets as fuel [5,6] and a higher heating value of the tars of ~29 MJ/kg was determined [7]. The LT-CFB design has low construction and maintenance costs and it can efficiently utilize troublesome marginal biomass resources with high contents of low melting ash compounds like straw, shea nut, seaweed and citrus peel residues, various manure and biogas residue fibers, and waste water sludge [8,9]. The LT-CFB technology has been proven to produce bio-ashes that were tested as soil amendments and showed good fertilizer properties and improved the quality of sandy subsoils [10–12].

Since the produced gas has a high tar content (>4.8 g/Nm^3) [13], it cannot be fed to gas engines or fuel cells without further gas cleaning. However, the problem of tar removal can be turned into an opportunity for liquid bio-fuel production, which is thereby proposed as a biomass based polygeneration plant that is able to co-produce heat, power, bio-oil and fertilizer (ashes) with very high overall efficiency and flexibility (see **Fig. 1**). The direct application of untreated bio-oil within existing infrastructure is impeded by its high oxygen content (17–50 wt.%) and acidity (pH = 2.5–3), resulting in undesirable properties such as low heating value, immiscibility with hydrocarbon fuels, thermal and chemical instability, high viscosity and corrosiveness [14,15]. Upgrading of bio-oils and reduction of the rather high oxygen content is hence required for efficient use of the oils and for the enhancement of oil properties. Upgraded bio-oil has many advantages, including higher stability, higher pH, simpler handling and various utilization possibilities as a high-load fuel for heat production, transportation, industrial processes or even as a gas turbine fuel for electricity production. Furthermore, the catalytic reactor and following tar condensation provide a tar free gas that can be utilized by an engine.

In contrast to catalytic cracking of gasifier tars for their complete decomposition [16–20], a milder tar deoxygenation and improvement of the fuel properties of the collected bio-oils was targeted in this work without severely reducing the bio-oil yield by the catalytic treatment. In-line atmospheric pressure catalytic upgrading of biomass pyrolysis vapors is one of the most promising and simple processes to produce upgraded bio-oils, and a wide variety of catalysts has been tested for this purpose in recent decades [21–29]. Catalytic upgrading of fast pyrolysis vapors can be conducted in a one-reactor system, where biomass is fed into a fluidized catalyst bed (often referred to as *in-situ* CFP [30,31]), or in a two-reactor system in which the catalytic upgrading is performed in a separate reactor downstream the pyrolysis reactor (*ex-situ* configuration [31,32]). While others have reported catalytic fast pyrolysis at larger scales from 2–40 kg/h biomass feeding rate [33–35], those units were operated in fast pyrolysis mode using woody biomass as feedstock with direct catalyst contact in a circulating fluidized bed. Compared to woody biomass, wheat straw contains a much higher content of alkaline ashes such as K, Ca, Cl and Mg. The direct contact with the catalyst in *in-situ* upgrading configuration can lead to transfer of the alkalines and poisoning of catalytic sites [34,36–38]. This led to patent applications involving the pretreatment of the biomass by washing and the washing out of ash deposits from the catalyst after oxidative regeneration [36,37], thereby adding complexity and costs.

The catalytic treatment reduces the oxygen content of the tars and converts some of the tar to permanent gas species. After the catalytic unit, the bio-oil can be collected from the producer gas (PG) by cooling and condensation and the product can be further treated in an oil refinery and be a potential substitute for traditional transport fuels (gasoline and diesel).

Amongst the catalysts tested, the zeolite catalyst HZSM-5 showed a good performance in terms of the production of aromatic hydrocarbons, deoxygenation and resistance to coke deposition, which can be attributed to the shape selectivity of its three dimensional pore structure and unique solid acidic characteristics. Recently, our group investigated the deoxygenation of wheat straw fast pyrolysis (FP) vapors over different HZSM-5, γ-Al_2O_3, and HZSM-5/γ-Al_2O_3 extrudates [39–41]. Due to the small size of HZSM-5 crystals (<1 μm), binders like alumina (γ-Al_2O_3) are required to shape the catalyst and ensure sufficient physical strength for both fixed bed and particularly fluid bed operation as well as catalyst transport and reactor filling. The alumina binder itself is acidic and is hydrothermally stable under typical reaction conditions of ~500 °C. The use of alumina for deoxygenation of biomass derived FP vapors [41–46] can offer economic advantages over HZSM-5 based catalysts, albeit higher coke yields and lower yields of aromatics result compared to HZSM-5 [41,42,47].

In this study, we performed catalytic upgrading of tars generated at a 100 kW_{th} low-temperature gasifier over HZSM-5/γ-Al_2O_3 and γ-Al_2O_3 in order to i) obtain information about the change in carbon distribution (condensable organics, gas, coke) and ii) to investigate the change in oil properties by detailed liquid characterization. The catalytic upgrading was performed in an *ex-situ* configuration using a side stream of the gasifier producer gas at a specifically designed test rig downstream the hot gas filtration of the vapors, which was found to further stabilize the bio-oil [48]. As the tars at the LT-CFB gasifier were generated at higher temperatures (~650 °C) compared to the usually reported FP temperature range of ~500-550 °C for maximum bio-oil yield [49], we further compare the properties of the bio-oils collected at the gasifier with “regular” FP oil generated at an ablative unit at 530 °C [39]. This investigation is the first of its kind to study catalytic upgrading of tars generated at an LT-CFB gasifier for collection of bio-oils with improved fuel properties.

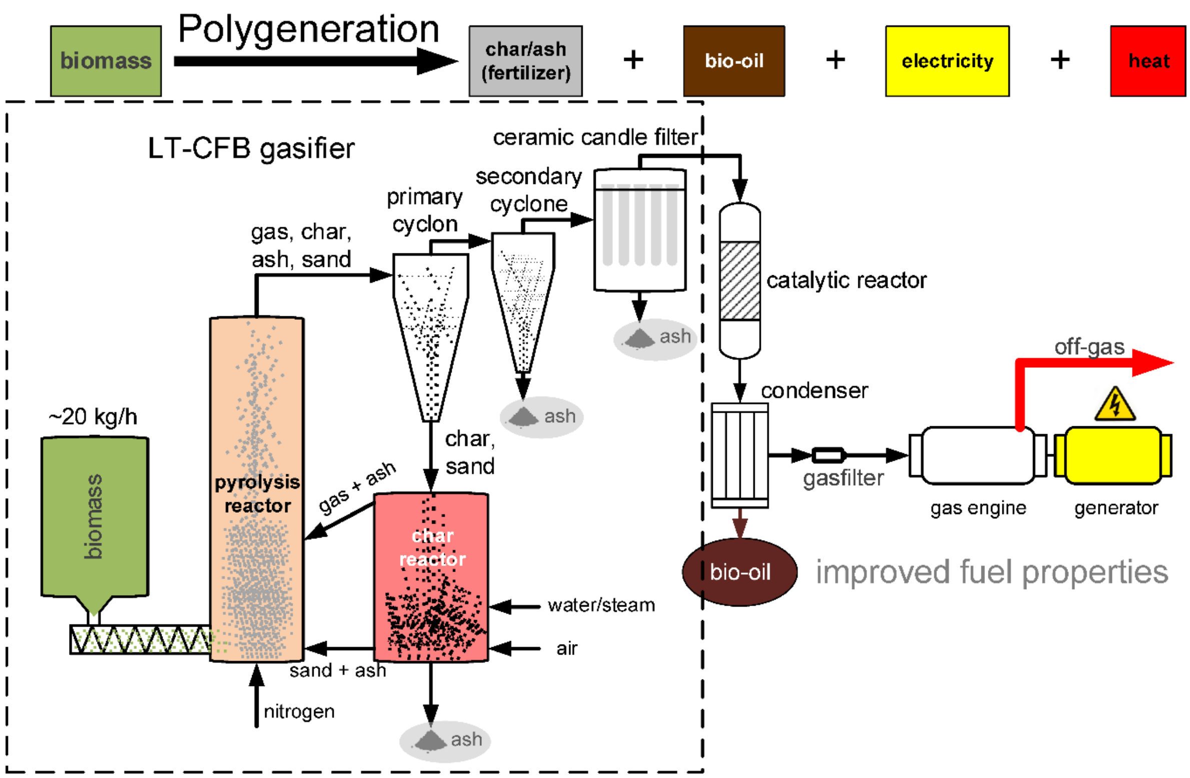

Fig. 1. Scheme of the LT-CFB gasifier (in dashed box) and proposed modification for polygeneration of char, bio-oil, electricity, and heat.

2 EXPERIMENTAL SECTION

2.1 Feedstock

The ultimate and proximate characterization of the Danish wheat straw pellets used as feedstock is shown in Table 1. The particle size of the crushed wheat straw pellets was <7 mm. The proximate and ultimate ash analysis by ICP and chlorine extraction was carried out by Force Technology, Denmark. The standard deviation of the N, C, H, and O (by difference) determination amounted to 0.02, 0.96, 0.11, and 1.06 wt%, respectively. The higher heating value (HHV) of the dry biomass was calculated to 17.7 MJ/kg based on the elemental composition and ash content of the biomass according to the formula reported by Channiwala and Parikh [50].

Table 1. Proximate and ultimate analysis of crushed wheat straw pellets used as feedstock.

Proximate analysis [wt%, as received]	
Moisture	8.5%
Volatiles	66.9%
Ash	6.6%
Fixed carbon (by difference)	17.9%

Ultimate analysis	
Elemental composition [wt%, daf]	
N	0.8%
C	46.2%
H	6.6%
O	46.4%
Inorganics [wt%, d.b.]	
Cl	0.11%
S	0.08%
Al	0.21%
Ca	0.32%
Fe	0.01%
K	0.98%
Mg	0.07%
Na	0.01%
P	0.11%
Si	1.10%

Sulfuric acid hydrolysis was used for the determination of carbohydrates bound in the cellulose and hemicellulose. Klason lignin was determined as the ash free residue after hydrolysis. First, 1.5 ml of 72% H_2SO_4 was added to 0.16 g sample and the sample was pre-hydrolyzed for 60 minutes at 30 °C. After dilution of the hydrolysate with MilliQ water (42 ml), the liquid samples were autoclaved at 120 °C for 60 minutes. Filtered liquids were analyzed on an HPLC column, while the solid residue was heated to 550 °C to determine the lignin ash content. The content of carbohydrates and Klason lignin was determined to be ~68.5 wt% and 20.2 wt%, respectively. The contribution of individual carbohydrates is listed in Table S1 (ESI).

2.2 Catalyst preparation

The extrudates of the γ-Al_2O_3 binder (same as used for preparation of the shaped HZSM-5/γ-Al_2O_3), and the HZSM-5/γ-Al_2O_3 extrudates consisting of 65% HZSM-5 (Si/Al ~40) and 35% Al_2O_3 binder were provided by Haldor Topsøe A/S. The shaped HZSM-5/γ-Al_2O_3 and γ-Al_2O_3 extrudates were downsized to a particle size of 250–850 μm. The catalysts were steamed prior to their use by injecting water (2 ml/min) into a preheated nitrogen stream (4 Nl/min) and passing the steam (~30 vol.-%) for 5 h through the fixed bed of catalyst kept at 500 °C under atmospheric pressure conditions.

30 g and 100 g of HZSM-5/γ-Al_2O_3 extrudates, 100 g of γ-Al_2O_3 extrudates, and 95 g of SiC were tested at ~500 °C. In addition, another test at lower catalyst temperature of ~450 °C was performed using 100 g of HZSM-5/γ-Al_2O_3 extrudates.

2.3 Catalyst characterization

The methodology for catalyst characterization has been outlined recently [39]. Ar physisorption was carried out using a Quantachrome AsiQ instrument for analysis of micro and mesopores. Prior to the measurement, samples were outgassed under vacuum at 350 °C overnight. The NLDFT model was applied to the adsorption branch of the Ar isotherm in order to determine the volume of micropores and mesopores. The specific surface area (S_{BET}) was calculated by the Brunauer-Emmett-Teller (BET) method. (V_{total}) was calculated from the amount of adsorbed nitrogen at the relative pressure of $p/p_0 = 0.95$.

Temperature programmed desorption (TPD) of ammonia was conducted at a Micromeritics AutoChem II Chemisorption Analyzer. For the individual treatment steps, the reader is referred to Eschenbacher et al. [39]. Curves were normalized using the sample mass. Based on a duplicate analysis, a standard deviation of 0.009 mmol NH_3/g was calculated.

Solid-state ^{1}H, ^{13}C and ^{27}Al NMR spectra were all recorded on a Bruker AVANCE III HD spectrometer operating at a magnetic field of 14.05 T (ν_{1H} = 600.165 MHz, ν_{13C} =150.911 MHz and ν_{27Al} = 156.384 MHz). The system was equipped with a 4 mm CP/MAS BBFO probe (Bruker) and the samples were spinning at 15 kHz for all experiments. For the ^{1}H and ^{27}Al NMR spectra a simple pulse-acquire experiment was employed using a 2.5 μs p/2 pulse with 5 s interscan delay for ^{1}H, and a 0.4 μs p/12 pulse with 0.5 s interscan delay for ^{27}Al. ^{13}C-{^{1}H} CP/MAS NMR spectra were acquired with a contact time of 2 ms, a ramped ^{1}H contact pulse and an interscan delay of 1 s. High-power ^{1}H SPINAL decoupling with ν_{RF} = 98 kHz was employed for both ^{27}Al and ^{13}C-{^{1}H} experiments. Chemical shifts are reported relative to neat TMS for ^{1}H and ^{13}C (δ = 0 ppm) and 1.0 M $AlCl_3$ (δ = 0 ppm) for ^{27}Al.

A detailed description of the ^{13}C and ^{1}H NMR analysis of fast pyrolysis oils was provided in our earlier work [39]. Resultant data were processed in TopSpin software (Bruker) using a Gaussian window function and re-plotted in Origin software for integration of the peak center bands.

Coke yields on the catalysts were determined by combustion of the coke in a thermogravimetric analyzer (Netzsch STA 449 F1 Jupiter ASC). About 50 mg of coked catalyst was filled in an alumina crucible. Using 40 ml/min total flowrate, the samples were first heated in nitrogen to 350

°C at 20 °C/min and held at 350 °C for 5 min in order to remove moisture. Secondly, the gas was adjusted to 20 vol-% oxygen by mixing 8 ml/min oxygen with 32 ml/min nitrogen and the temperature was held for an additional 5 min at 350 °C before ramping to 700 °C at 10 °C/min and holding the final temperature for 10 min.

2.4 Bio-oil characterization

All liquid products were kept refrigerated at 5 °C. A detailed description of methods applied for oil characterization can be found in our earlier work [39]. In brief, the collected oil and aqueous fractions were analyzed for moisture content by Karl Fischer titration (ASTM E203-08) and elemental composition (nitrogen, carbon, hydrogen) was measured using an EA3000 CHNS elemental analyzer from Eurovector. Prior to analysis, 1-3 mg of sample was sealed in tin capsules. Calibration (R^2 = 0.998) was performed with acetanilide (>99%) and sulphanilamide (>99%). A minimum of two replicates were performed per sample. As the sulfur concentration was below the detection limit of the elemental analyzer, oils were subjected to total sulfur analysis according to ASTM method D5453. The oxygen content was determined by difference. Taking into account the moisture content, the elemental composition of the dry organics was calculated. The higher heating value of the bio-oil (d.b.) was calculated based on the elemental composition using an empirical formula according to Channiwala and Parikh [50]. The phase separated oil and aqueous fraction were analyzed using a GC-MS/FID Shimadzu QP 2010 Ultra apparatus equipped with a Supelco Equity 5 column. Identification and quantification of the species in the samples was performed by the mass spectrometer and flame ionization detector (FID), respectively. Aqueous samples were analyzed directly while the oil samples were diluted in a 1:9 volumetric ratio in acetone. The initial temperature for the GC column was held at 40 °C for 10 min and the column was heated up to 250 °C with an initial heating rate of 2 °C/ min up to 100 °C followed by an increased heating rate of 8 °C/min. A split ratio of 80 was used at the injection. The MS scanning was set to a range of 20 to 300 m/z. For calculation of relative FID areas, the effective carbon number method outlined by Schofield was applied [51].

The organic-rich oil fractions were further analyzed for total acid number (TAN) according to ASTM D 664 using an 848 Titrino plus (Metrohm). The accuracy was verified by analyzing an ASTM standard with 10 mg KOH/g (Paragon Scientific Limited). The basic nitrogen content of the oils was analyzed following the UOP Method 269-10 for determination of nitrogen bases in hydrocarbons by titration. Size exclusion chromatography was performed according the details described in earlier work [39].

To investigate the reactivity and charring behavior of the collected bio-oils during reheating, the evaporation behavior of the oils was investigated in a thermogravimetric analyzer (Netzsch STA 449 F1 Jupiter ASC). After weighing of an empty Pt crucible with perforated lid, 10–20 mg of oil was placed into the crucible immediately before the sample was weighed and the heating ramp started. The temperature was ramped at 10 °C/min to 500 °C under N_2 atmosphere and held at the final temperature for 30 min.

In order to analyze the chemical composition of the whole oils, selected oils were subjected to ^{1}H, ^{13}C NMR and 2D HSCQ NMR analysis. Details of the used instruments and experimental conditions are provided in earlier work [39]. For integration of the quantitative ^{13}C NMR spectra of FP oils and catalytically treated FP oils, the recommendations from Happs et al. [52] were followed.

2.5 Experimental set-up of LT-CFB gasifier

The plant concept and operating principle of the LT-CFB gasifier is described in more detail in several references [3,4,6,9,12,53,54], and a photograph of the 100 kW_{th} unit is provided in Fig. S1. Since the sum of the gasses from gasification and pyrolysis is passing through the upper part of the pyrolysis reactor and since the square section of the pyrolysis chamber is much smaller than for char gasification, the gas velocity in the pyrolysis chamber is much higher than in the gasification chamber. As such, the char is gasified in a slowly fluidized bubbling bed type reactor while pyrolysis takes place in a fast bed type reactor, wherein the added gas from the char gasifier constitutes a large part of the upwards gas flow. This design has several benefits:

1) A lower char gasification temperature (to avoid agglomeration problems) by achieving better char retention than would be possible in a more usual large scale one-chamber CFB reactor,

2) An even lower pyrolysis temperature to avoid secondary pyrolysis reactions (that would expand the gas volume and produce soot and polycyclic aromatic hydrocarbons),

3) Making the pyrolysis reactor act as an in situ—alkaline condensing—raw gas cooler, so that also the alkalines evaporated in the char reaction chamber can be efficiently retained by simple down stream particle separation,–i.e. without the need for inserting an expensive raw gas cooler, preventing heat loss as well as potential corrosion and deposition problems.

The biomass feeding-rate in this work was ~20 kg/h and the weight of the feeder was continuously monitored. In addition, the flow of nitrogen, air, and water into the system was recorded. The temperature of the pyrolysis chamber was measured at seven, vertically distributed positions. Within this work, the average temperature of those measurements is reported. For three closely located pyrolysis temperatures (663, 659, and 665 °C), the uncertainty in tar load of the producer gas (expressed as standard deviation) was 0.8 g/Nm^3 for the tar recovered as bio-oil.

Experiments in this study were performed by withdrawing a side stream of ~2% from the LT-CFB producer gas. For the investigations on the effect of temperature of the LT-CFB pyrolysis chamber on the tar loading in the producer gas and the bio-oil quality, a cooling-water based one-stage condensation device as described by Thomsen et al. [9] was used. For further experimental details, the reader is referred to Jensen [55].

In order to determine the change in product distribution and properties by the catalytic treatment, a new test rig was designed which comprised two parallel condensation trains. This allowed parallel condensation of tars and collection of dry gas for both the raw producer gas and the tars after catalytic treatment, as shown in **Fig. 2**. The first condensation stage consisted of a series of metal impingers cooled to 4 °C. As second stage an electrostatic precipitator (ESP) was operated at room temperature. The third condensation stage consisted of a series of glass impingers cooled to −60 °C by an external dry ice/ethanol bath. The liquid collected at the ESP was a single-phase oil whereas the liquid collected at the first and third step spontaneously phase separated into an organic rich and an aqueous fraction. The three different oil fractions and two different aqueous fractions were combined to a single oil and an aqueous liquid, respectively. The time of the experiment was recorded and the total volume of the sampled non-condensable gas was measured by the cumulative flow meters.

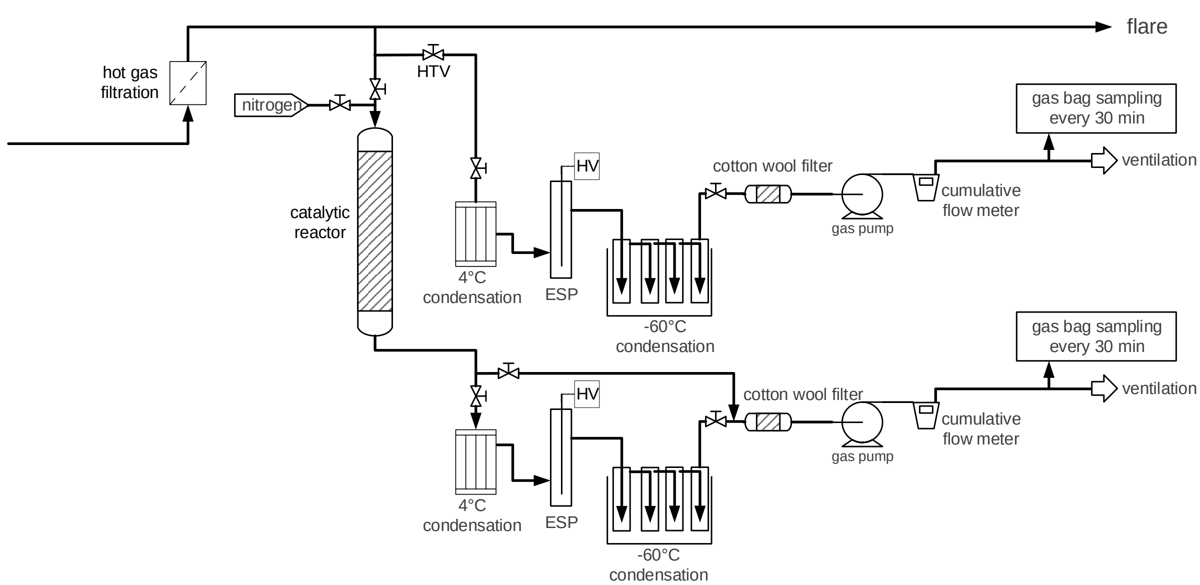

Fig. 2. Test rig with two parallel condensation trains for condensation of tars and dry gas sampling.

For the test of 30 g of HZSM-5/γ-Al_2O_3 catalyst, an externally heated reactor tube (ID = 20 mm, length = 190 mm) was used resulting in a catalyst bed volume of ~60 ml. A larger externally heated reactor (ID = 67 mm, length = 250 mm) was used for tests with 100 g of catalyst. Quartz wool and perforated distribution plates were placed between the catalyst bed and the gas inlet and outlet in order to ensure plug flow behavior and avoid channeling or dead pockets. For both reactor dimensions, the temperature of the catalyst bed was measured by thermocouples in the center of the bed. The flow rate of dry gas was ~9 Nl/min for the large reactor bed (100 g catalyst) while it was ~3 Nl/min for the narrower reactor due to the increased pressure drop of the bed. The corresponding weight hourly space velocity based on the vapor products to the catalyst fixed bed is estimated to be 1.9 g tar per g catalyst per hour [h^{-1}] for the small reactor scale. When using 100 g of catalyst the WHSV was in the range of 0.5-1 h^{-1} based on the variations in the tar concentration of the producer gas. Upon contact of the catalyst with tars, the temperature of the catalyst increased by 30-40 °C (see temperature profile measured by thermocouple in center of reactor bed, Fig. S2), after which the temperature slowly decreased. This indicates the occurrence of exothermic reactions upon contact of the tars with the acid sites of the catalyst. The catalytic treatment was followed by rapid quenching of the vapors in a condensation train consisting of dry operated metal impingers (4 °C), an electrostatic precipitator (25 °C), and several dry operated glass impingers (-60 °C). Samples of the non-condensable gasses were filled into gas bags and analyzed off-line with a gas chromatograph (Thermo Scientific refinery gas analyzer, Trace 1300/1310) equipped with a flame ionization detector (FID) and two thermal conductivity detectors (TCD), which measured the gas composition (H_2, N_2, CO, CO_2, C_1 to C_5, and C_{6+} hydrocarbons). Chromeleon Chromatography Studio software was used for analysis of the chromatograms.

3 RESULTS AND DISCUSSION

3.1 Catalyst properties

The physicochemical characteristics of the steamed HZSM-5/γ-Al_2O_3 and γ-Al_2O_3 catalysts were recently reported in our earlier work [41]. An overview of important properties is given in

Table 2. While γ-Al_2O_3 is purely mesoporous, the HZSM-5/γ-Al_2O_3 extrudates had a microporous volume (V_{micro}) of 0.11 cc/g due to the zeolite component. It is further noteworthy that the zeolite containing catalysts contained more Brønsted acidity compared to γ-Al_2O_3. **Table 2** further contains the textural properties of two coked catalysts from the in-line tar treatment at 500 °C. For both HZSM-5/γ-Al_2O_3 and γ-Al_2O_3 the coke deposition reduced the surface area. The coke deposition on Al_2O_3 reduced the total pore volume V_{total} from 0.53 to 0.36 cc/g and a shift to narrower power width can be observed from the pore size distribution, which is attributed to the coke deposition in mesopores (see Fig. S3). Similarly, the V_{micro} and the volume of mesopores V_{meso} of HZSM-5/γ-Al_2O_3 decreased due to the coke deposition. While not further investigated in this work, a significant reduction in acidity due to the coke deposition can be expected as observed for upgrading of wheat straw FP vapors generated at lower temperature of 530 °C over HZSM-5/γ-Al_2O_3 [41].

Table 2. Physicochemical properties of the steamed and coked HZSM-5/γ-Al_2O_3 and γ-Al_2O_3 catalysts. For the coked catalysts, the processed amount of tar per g catalyst was 1.02 and 0.74 g/g for HZSM-5/γ-Al_2O_3 and γ-Al_2O_3, respectively. Textural properties were determined by high-resolution low temperature Argon physisorption (87 K), total acidity and Brønsted acidity was determined by TPD of NH_3 and Ethylamine respectively, as described in Eschenbacher et al. [40].

	HZSM-5/γ-Al_2O_3	γ-Al_2O_3	coked HZSM-5/γ-Al_2O_3	coked γ-Al_2O_3
$V_{micro}{}^{a}$ [cc/g]	0.11	0	0.09	0
$S_{micro}{}^{a}$ [m^2/g]	859	0	665	0
$V_{meso}{}^{a}$ [cc/g]	0.28	0.52	0.15	0.33
$S_{meso}{}^{a}$ [m^2/g]	171	268	78	183
V_{total} at p/p_0 =0.95	0.45	0.53	0.30	0.36
BET area (Ar) [m^2/g]	376	192	235	174
Acidity^{b} [mmol NH_3/g]	0.39	0.31	n.d.	n.d.
Brønsted acidity^{c} [mmol NH_3/g]	0.15	0.06	n.d.	n.d.

^{a}obtained by applying NLDFT method to adsorption branch of isotherm; ^{b}determined by NH_3-TPD; ^{c} Brønsted acidity was quantified by TPD of ethylamine [40] .

The ^{27}Al solid-state NMR spectra of HZSM-5/γ-Al_2O_3 prior to catalytic use (**Fig. 3**a) shows a high fraction of AlO_6 (-5-10 ppm), which can be attributed to i) the mostly Lewis acidic γ-Al_2O_3 binder, and ii) the transformation of tetrahedral framework AlO_4 (54 ppm) in the HZSM-5 zeolite to extra-framework aluminate domains of AlO_5 (20-30 ppm) and AlO_6 (-5-10 ppm) by the steam treatment prior to catalytic testing. Overall, for HZSM-5/γ-Al_2O_3 the contribution of extra framework Al did not significantly change by the catalytic test and coke deposition (67.2% before and 68.0% after the catalytic test). The coked γ-Al_2O_3 catalyst on the other hand showed a slightly higher contribution of extra framework Al (69.3%) compared to HZSM-5/γ-Al_2O_3.

^{13}C NMR of the coked catalysts (**Fig. 3**b) revealed that generally the nature of the coke species deposited on γ-Al_2O_3 and HZSM-5/γ-Al_2O_3 is quite similar. In both cases, the coke is highly aromatic, as shown by the peak at ~125 ppm and the two spinning side bands at ~225 and ~25 ppm. In addition, both coked catalysts exhibit distinct shoulder peaks at ~150, 145, 140 and 120 ppm, which indicate the presence of several aromatic species and possibly also olefin structures. Both catalysts further show a peak at ~20 ppm, which is attributed to aliphatic groups. This feature is better defined for the coked HZSM-5/γ-Al_2O_3 catalyst compared to the coked γ-Al_2O_3 catalyst, in agreement with ^{1}H NMR (see feature at ~3 ppm, Fig. S4). Due to the relative high spinning speed, the areas of the 1st order aromatic sidebands in ^{13}C NMR can be assumed to be almost identical. Subtracting the area of the side band at ~225 ppm from the convoluted peaks in the range 50-0 ppm thus allows estimating the contribution of the aliphatic peak. The ratio of the aliphatic-to-aromatic carbon contribution was thus estimated to 12.7% and 5.8% for the coked HZSM-5/γ-Al_2O_3 and γ-Al_2O_3 catalyst, respectively.

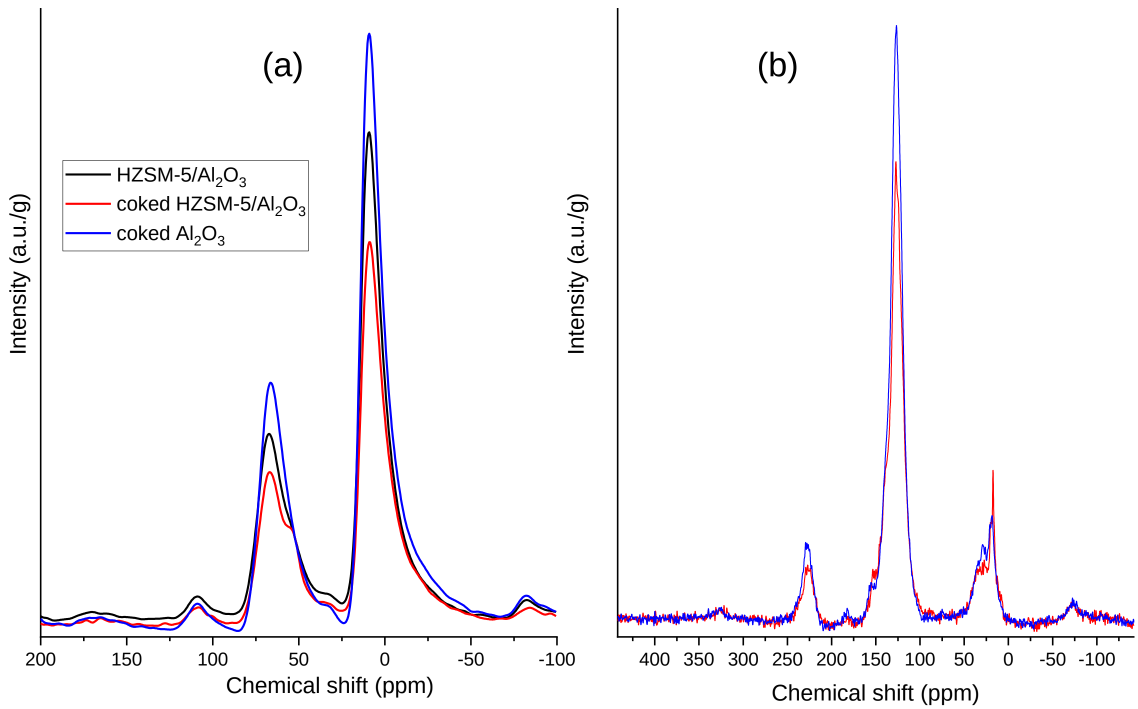

Fig. 3. (a) ^{27}Al solid-state nuclear magnetic resonance spectra of the HZSM-5/γ-Al_2O_3 prior to catalytic use, and the coked versions of HZSM-5/γ-Al_2O_3 and γ-Al_2O_3 after in-line catalytic treatment (500 °C) of LT-CFB producer gas from wheat straw. (b) ^{13}C NMR of the coked versions of HZSM-5/Al_2O_3 and Al_2O_3. Signals are normalized by sample mass (dry). Legend in **Fig. 3**(a) also applies for **Fig. 3**(b).

3.2 Mass balance

The amount of biomass, nitrogen, air, and water fed into the LT-CFB during the sampling of the PG side stream was recorded. By taking the inflow of nitrogen as an internal standard, the mass balance for the LT-CFB operation could be closed to ~95-122%. The raw mass balance data is provided in Tables S2-S6. Note that the char yield could not be determined. However, since the mass balance closure was close to or above 100% in most tests, it appears that no char accumulation had occurred in the char combustion reactor while the producer gas was sampled. Mass balance above 100% during the PG sampling period can be explained if the air that was fed into the system not only combusted the chars produced from the biomass, but also converted some char that had accumulated prior to the sampling period in the char combustion reactor.

Table 3 shows the product yields with respect to the sum of biomass (dry and ash-free) and oxygen fed to the LT-CFB for the sampling of raw (un-treated) producer gas and after in-line catalytic treatment. Generally, the vapor treatment reduced the yield of organics recovered in the phase-separated oil phase, increased the gas yield and produced coke. For unknown reasons, the reaction water obtained without catalyst at a LT-CFB pyrolysis temperature of 626 °C was unusually low compared to the other tests, but unfortunately it was not possible to repeat the test. The yield of bio-oil on the other hand is in line with the values from the other experiments.

The coke yield on γ-Al_2O_3 was higher compared to HZSM-5/γ-Al_2O_3, in agreement with literature [41]. While the coke yields were shown to increase with catalyst temperature for γ-Al_2O_3 and mesoporous HZSM-5/γ-Al_2O_3 [41] when treating FP vapors generated at 530 °C, the coke yield was slightly higher when treating LT-CFB vapors at a catalyst temperature of 450 °C (2 wt%) compared to 500 °C (1.6 wt%). This is attributed to the fact that less tar was processed over the catalyst at 450 °C (0.67 g tar/g catalyst) compared to 500 °C (1.0 g tar/g catalyst), and it is known that higher coke yields result at lower ratios of fed biomass-to-catalyst and processed tar/g catalyst.

It was further observed that the yield of organics recovered in the aqueous fraction decreased upon treatment with HZSM-5/γ-Al_2O_3 and γ-Al_2O_3 at 500 °C, while it remained unchanged at a lower catalyst temperature of 450 °C (HZSM-5/γ-Al_2O_3). This observation is attributed to a higher polarity of the condensed organics at lower catalyst temperature and thus a higher recovery in the aqueous phase. The trend agrees with a higher TAN (15 mg KOH/g) of oil obtained at 450 °C catalyst temperature while oils obtained at a catalyst temperature of 500 °C showed a lower TAN (3-5 mg KOH/g).

Table 3. Product yields (except char) with respect to the sum of biomass (dry and ash-free) and oxygen fed to the LT-CFB during the sampling period.

$T_{pyrolysis}$ [°C]	Catalyst ($T_{catalyst}$)	Organics (oil phase)	Organics (aq. phase)	Reaction water	Gas (incl. C_4+)	Coke	Mass balance [%]
626	-	10.0%	5.6%	10.4%	73.9%	0.0%	100%
	HZSM-5/γ-Al_2O_3 (450 °C)	9.3%	5.3%	20.5%	74.3%	2.0%	111%
656	-	8.9%	7.4%	23.1%	76.7%	0.0%	116%
	HZSM-5/γ-Al_2O_3 (500 °C)	8.3%	3.9%	19.8%	82.5%	1.6%	116%
662	-	9.3%	2.8%	19.9%	73.4%	0.0%	115%
	γ-Al_2O_3 (500 °C)	6.9%	1.9%	24.2%	76.5%	3.0%	112%

3.3 Gas composition

The dry producer gas contained 53-58 vol.% N_2. The other main gas components present in the LT-CFB producer gas were CO_2 (19-22 vol%), CO (12-17 vol%), hydrogen (4-6 vol%), and methane (3-5 vol%).Table 4 lists the nitrogen-free gas composition. It appears that with increasing temperature in the pyrolysis chamber, the selectivity to methane/ethane and CO increased. Upon contact of the tar vapors with the acidic catalysts, the concentrations of olefins (ethylene and propene) increased in the initial vapor-upgrading phase. With ongoing time on stream and catalyst deactivation, the concentration of olefins decreased. Increased yield of olefins in the initial vapor upgrading phase was also observed for in-line catalytic treatment of wheat straw FP vapors generated at 530 °C with HZSM-5/γ-Al2O3 and γ-Al2O3 [41]. Averaged over the gas-sampling period, the olefin concentration was increased by the catalytic treatment, especially for propene (Table 4).

Table 4. Gas composition in vol% on N_2-free basis

		Methane	Ethane	Ethene	Propane	Propene	CO_2	CO	Hydrogen	C_4+
626	-	7.1	0.8	1.4	0.1	0.8	50.7	26.9	11.5	0.6
	HZSM-5/γ-Al_2O_3, 450 °C	6.8	0.8	2.0	0.1	1.7	50.6	26.8	10.6	0.7
656	-	7.5	0.7	1.9	0.1	0.9	45.9	28.3	14.0	0.6
	HZSM-5/γ-Al_2O_3, 500 °C	7.8	0.8	2.4	0.1	1.5	45.5	29.0	12.2	0.7
662	-	9.2	0.9	2.2	0.1	1.0	39.8	34.8	11.3	0.7
	γ-Al_2O_3, 500 °C	9.9	1.0	2.5	0.1	1.2	40.3	36.0	8.2	0.7
671	SiC	8.7	0.8	2.4	0.1	1.0	46.4	29.8	10.0	0.8
660	HZSM-5/γ-Al_2O_3, 500 °C	8.6	0.9	2.2	0.1	1.1	45.1	29.7	11.7	0.7

3.4 Product distribution and bio-oil quality

Table 5 provides an overview of the average temperature in the pyrolysis chamber of the LT-CFB during the tar sampling period. In addition, the used catalyst masses and temperatures are indicated. It should be noted that for the first two columns of Table 5 the sampling of raw and catalytically treated tars was performed on two adjacent days and not in parallel as for the remaining columns of Table 5. As a result, for the first two columns of Table 5 the pyrolysis temperature of the gasifier was not identical during the sampling of raw and treated tars. In addition, it should be noted that catalytic upgrading was performed with only 30 g of catalyst and that the reactor was filled with SiC to obtain an inert reference. The tests performed with parallel sampling of raw and treated PG (columns three to eight of Table 5) were performed with 100 g of catalyst and the untreated reference bio-oil was obtained without being passed over a hot bed of SiC.

Using 100 g HZSM-5/γ-Al_2O_3 at 500 °C in the catalytic treatment reduced the tar load by 18%. Upon reduction of the catalyst temperature to 450 °C, the tar load in the PG decreased only slightly by 3%. The highest reduction in tar load (by 24%) was observed using 100 g γ-Al_2O_3. The more pronounced decrease in tar loading for γ-Al_2O_3 can be attributed to its higher selectivity for coke formation, as will be discussed in section 3.5. An effect of pyrolysis temperature on the tar load is observed as the tar load decreased from 134 to 92 g/Nm^3 when increasing the average pyrolysis temperature from 626 °C to 671 °C.

The inline catalytic treatment of the tars influenced the carbon distribution of the producer gas, as can be observed for the results obtained with parallel sampling. The carbon contribution of condensable organics decreased by 27 and 25 % when using 100g of γ-Al_2O_3 and HZSM-5/γ-Al_2O_3 while it only decreased by 12% (from 57 to 50%) when lowering the catalyst temperature to 450 °C for HZSM-5/γ-Al_2O_3. Up to ~10% of the carbon in the producer gas formed coke on the catalyst.

In all cases, the inline catalytic treatment of the producer gas improved the fuel properties of the collected liquid. The oxygen content was decreased to 10-12 wt% O (d.b.) from a raw bio-oil oxygen content of 14-18 wt% O along with a decrease in moisture content to ~3 wt% and an increase in higher heating value to a maximum of 35.5 MJ/kg. In addition, the TAN—which is an important indicator for the corrosiveness of fuels—could be significantly reduced by 51–92% compared to the untreated reference oils. Similarly, a reduction in basic nitrogen content was observed after catalytic treatment compared to the untreated reference oils. Vapor upgrading over 100 g HZSM-5/γ-Al_2O_3 catalyst reduced the basic nitrogen content by ~0.3 mass%, both at a catalyst temperature of 450 and 500 °C (see **Table 5**). γ-Al_2O_3 on the other hand only achieved a reduction by ~0.1 mass%. It is interesting to note that this behavior is opposite to what was observed for upgrading of fast pyrolysis vapors generated at a lower temperature (530 °C) using the HZSM-5/γ-Al_2O_3 catalyst, which led to an increase in basic nitrogen content from 0.39 to 0.57 mass% [56]. The observed increase in basic nitrogen by catalytic deoxygenation of FP vapors generated at 530 °C and the increase in basic nitrogen with increasing FP temperatures observed at the LT-CFB could indicate that basic nitrogen compounds are less prone of being converted compared to oxygenates.

The weight loss curves during heating of the oils in a TGA are provided in Fig. S5 (ESI). The catalytic treatment of the tars reduced the reactivity and charring propensity of the oils. This is indicated in Table 5 by comparing the mass remaining at 300 and 500 °C with respect to the initially loaded content of dry organics contained in the oils. The improved revaporization after catalytic treatment can be attributed to cracking and deoxygenation reactions, and it can be noted that the cracking was more severe when loading 100 g of catalyst as opposed to 30 g and operating at 500 °C as opposed to 450 °C. In addition, the reduced catalyst temperature of 450 °C catalyst temperature was less effective in reducing the TAN of the collected oil. The oil characterization by size exclusion chromatography (SEC) shown in Fig. S6 revealed that compared to the fast pyrolysis bio-oil obtained at 530 °C the LT-CFB oils obtained at 620-660 °C contain a relatively higher contribution of light MW compounds. This is likely due to cracking reactions occurring at the increased pyrolysis temperature. The tar treatment of the LT-CFB vapors with HZSM-5/Al_2O_3 at 450 °C did only slightly increase the contribution of low MW compounds, while a more pronounced additional cracking to lower MW was achieved at a catalyst temperature of 500 °C.

Table 5. Overview of temperatures in the pyrolysis chamber of LT-CFB, relative carbon product distribution of the producer gas, and key properties of the condensed bio-oil (phase separated from aqueous phase).

average T pyrolysis chamber [°C]	671	660	662		656		626	
Catalyst, Temperature	SiC, 500 °C	HZSM-5/γ-Al_2O_3, 500 °C	-	γ-Al_2O_3, 500 °C	-	HZSM-5/ γ-Al_2O_3, 500 °C	-	HZSM-5/ γ-Al_2O_3, 450 °C
Mass [g]	95	30	-	100	-	100	-	100
Processed tar g/g catalyst		1.75		0.74		1.02		0.67
Flowrate dry gas (after condensation) [Nl/min]	2.4	3.1	6.9	8.6	8.3	6.7	8.8	9.1
Tar in producer gas [g organics/Nm^3 dry gas]	92	137	98	74	123	101	134	125
Carbon distribution condensable organics/gas/coke*	25/75/0	37/61/2	26/74/0	18/75/7	27/73/0	22/75/4	30/70/0	28/67/5
Properties of bio-oil								
H_2O content [wt%]	6.2	3.00	8.10	2.50	9.90	2.70	16.60	4.10
wt% N (d.b.)	3.0	4.4	3.6	4.3	3.1	3.5	3.9	2.2
wt% C (d.b.)	68.4	76.1	75.1	77.8	76.7	78.5	70.8	78.0
wt% H (d.b.)	7.5	7.7	7.2	7.9	7.6	7.3	7.4	8.1
wt% S (d.b.)	0.29	0.28	0.45	0.50	0.32	0.21	0.36	0.16
wt% O (d.b., by diff.)	21.2	11.8	14.1	10.0	12.6	10.7	17.8	11.7
HHV [MJ/kg]	30.5	34.4	33.2	35.4	34.3	34.9	31.6	35.5
O/C	0.24	0.12	0.14	0.10	0.12	0.10	0.19	0.11
H/C	1.31	1.21	1.14	1.22	1.18	1.11	1.25	1.24
TAN [mg KOH/g]	25.2	12.3	14.1	4.7	33.9	2.8	35.2	15.0
Basic nitrogen [mass%]	1.24	1.20	1.3	1.2	0.7	0.4	0.6	0.3
Solid remains [wt% d.b.] at 300 °C/500 °C	36/11	32/8	38/11	19/3	39/16	18/6	42/17	25/8

*Carbon in char not included

Comparing the tar load and the carbon distribution of the raw producer gas as well as the quality of the obtained tars in **Table 5** indicates a significant influence of the average temperature of the pyrolysis chamber of the gasifier. With decreasing pyrolysis temperature, the carbon contribution of condensable tars in the producer gas increased while the carbon contribution of light gases in the producer gas decreased. To further investigate this aspect, the relative carbon distribution in the LT-CFB producer gas (excluding carbon retained in char) was compared to FP results obtained at an ablative bench scale FP unit [39] for the same feedstock as shown in Table S7. The inline catalytic treatment lost carbon to coke on the catalyst and reduced the recovery of producer gas carbon in the form of condensable bio-oil and aqueous phase. The latter is usually considered as wastewater since the recovery of the dissolved oxygenates from the aqueous phase is challenging, but research is ongoing in this field [57–60]. By taking nitrogen as an internal standard for the sampling of the producer gas slip stream, the carbon yields with respect to the total fed biomass could be calculated (see Table S8). The carbon yield (relative to fed biomass) of phase separated bio-oil and C_4+ components in the gas was clearly lower at ~21-22 wt% C at the LT-CFB (pyrolysis temperature 630-660 °C) compared to ~34 wt% C using an ablative fast pyrolysis unit at 530–550 °C [39]. However, also the amount of carbon lost to the aqueous stream decreased from ~12 wt% C at 530–550 °C to as low as 3.5 wt% C for the highest LT-CFB pyrolysis temperature of ~660 °C. The char yields could not be determined for the LT-CFB tests, but it is clear from Table S8 that in contrast to regular fast pyrolysis systems, the char gasification at the LT-CFB lead to more of the fed carbon being contained in the dry gas. Several aspects contribute to uncertainty in the carbon mass balance. Some uncertainty arises due to the larger scale of the system. Effects such as carbon accumulation (explaining carbon balances below 100%) or higher carbon gas yields due to increased char gasification (explaining carbon balances above 100%) can occur.

While the oil yield decreased by the catalytic treatment, a clear improvement in the properties of the collected bio-oils was observed. The reduced carbon losses to the aqueous phase after catalytic vapor upgrading seen in Table S8 agrees with the results obtained in the ablative bench scale FP set-up [39–41]. It should be noted that more carbon was recovered as aqueous phase at lower pyrolysis temperatures in the LT-CFB, in agreement with observations from bench scale ablative fast pyrolysis. In addition, it was observed that inline treatment of the LT-CFB tars with a catalyst temperature of 450 °C did not reduce the carbon lost to the aqueous phase, while it was more effectively decreased at a catalyst temperature of 500 °C. This is attributed to increased cracking of polar, oxygen-containing compounds at the higher catalyst temperature, which lowered the polarity of the condensed tars and thus the extent of solvation into the aqueous phase.

With increase in the temperature of the pyrolysis chamber, the carbon distribution in the producer gas shifted towards more light gas at the expense of condensable organics (including C_4+ measured in the gas phase) and organics recovered in the aqueous phase. The trend in production distribution with pyrolysis temperature agrees with results obtained with the same feedstock at an ablative bench scale FP unit (feeding rate ~0.2 kg/h) at lower pyrolysis temperatures of 530 and 550 °C [39], as shown in in **Fig. 4**.

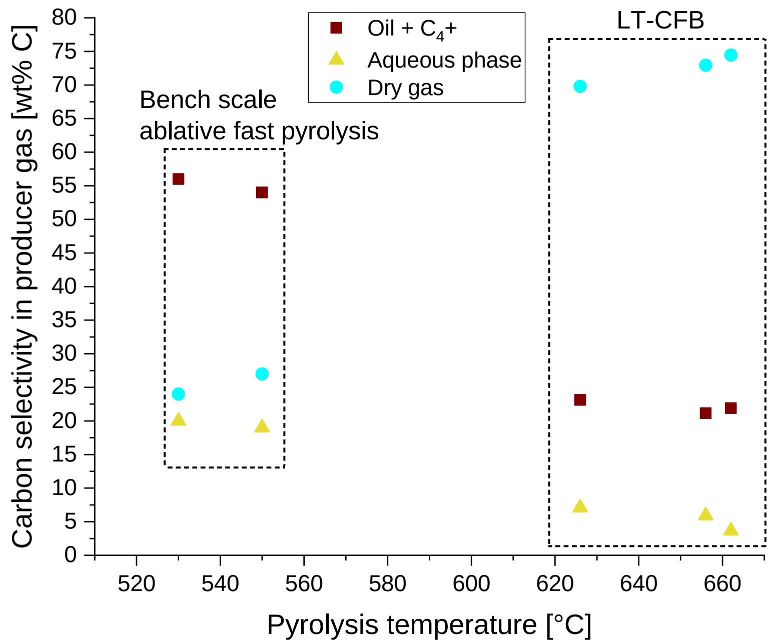

Fig. 4. Carbon distribution (excluding char) in raw producer gas obtained from LT-CFB gasification and ablative bench scale fast pyrolysis of wheat straw as a function of temperature.

Based on the determined mass yields (**Table 3**) the energy recovery of condensable organics was calculated taking into account the heating values (calculated based on elemental composition) of the condensed oil phase, aqueous phase, and C_4+ components measured in the gas phase. The deoxygenation using HZSM-5/γ-Al_2O_3 hardly affected the energy recovery of condensable organics. As illustrated for a catalyst temperature of 450 °C, this can be attributed to the fact that the organics content in the producer gas was only slightly reduced by the catalytic treatment from 134 g/Nm^3 to 125 g/Nm^3, but the HHV of the condensed oil phase (containing about 2/3 of the energy content of condensables) increased from 32 to 35 MJ/kg. A higher penalty in the energy recovery of condensable organics was observed when using γ-Al_2O_3 compared to HZSM-5/γ-Al_2O_3 at 500 °C, which is attributed to the higher coking propensity of γ-Al_2O_3.

Table 6. Energy recovery of condensable organics with respect to fed wheat straw.

$T_{pyrolysis}$ [°C]	Catalyst ($T_{catalyst}$)	Organics (oil phase)	Organics (aq. phase)	C_4+ in gas	sum
626	-	21.3%	9.9%	2.8%	34.0%
	HZSM-5/γ-Al_2O_3 (450 °C)	22.4%	9.3%	2.1%	33.7%
656	-	21.7%	7.3%	2.8%	31.8%
	HZSM-5/γ-Al_2O_3 (500 °C)	20.1%	7.1%	3.4%	30.6%
662	-	20.1%	4.8%	3.5%	28.4%
	γ-Al_2O_3 (500 °C)	15.9%	3.4%	2.9%	22.2%

The effect of the pyrolysis temperature on the product distribution in the producer gas that was observed by using the three-stage condensation system agrees with investigations by Jensen [55] who used a simpler condensation setup as described by Thomsen et al. [9]. **Fig. 5** shows that with increasing pyrolysis temperature, both the oil phase and the aqueous phase decreased. **Fig. 6** compares the determined tar load (g of dry organics per Nm^3 dry gas) using the one-stage condensation system described by Thomsen et al. [9] with the tar load determined by using a three-stage condensation system which includes an ESP for collection of aerosols and a dry ice trap for collection of light compounds [39]. Clearly, more tar was recovered using the latter condensation apparatus, which was applied in this work. This can be explained by an inefficient collection of aerosols and compounds with low boiling point temperature using the one-stage condensation system. Nevertheless, similar conclusions for the quality of the collected bio-oil could be obtained using the simple condensation system; with increasing pyrolysis temperature, the moisture content of the oil phase decreased while its higher heating value increased (see **Fig. 7** and **Table 5**).

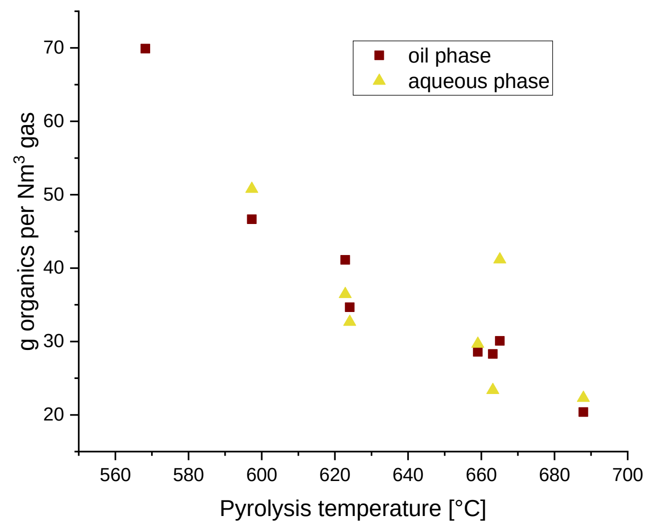

Fig. 5. The effect of pyrolysis temperature on the amount of condensed organics recovered in the phase-separated oil and aqueous fractions. Data obtained with simple one-step condensation.

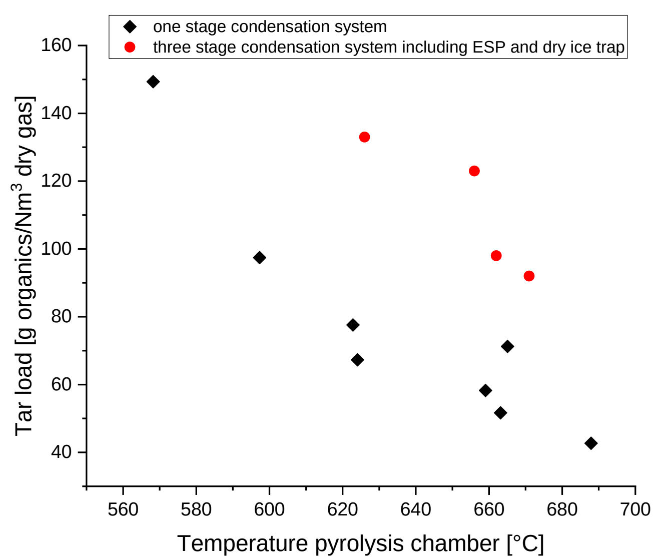

Fig. 6. Comparison of tar loads determined by tar condensation using a one-stage condensation system (♦) and tar loads determined using a three stage condensation system (•).

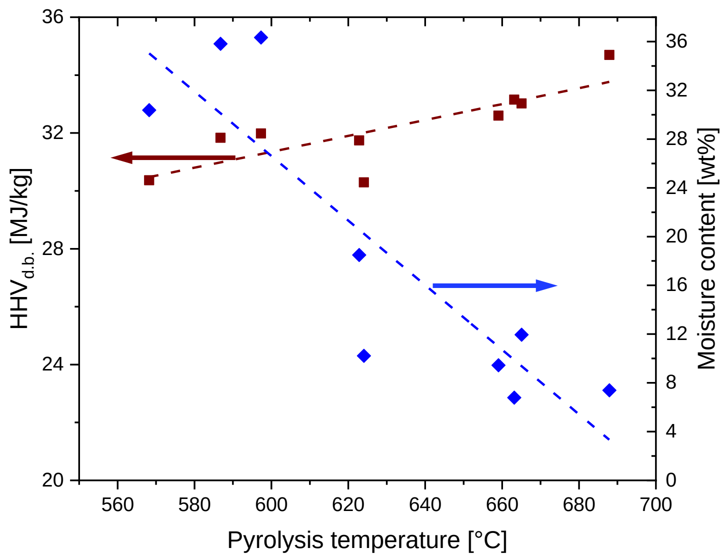

Fig. 7. The effect of pyrolysis temperature on the moisture content in the collected bio-oil and the higher heating value (on dry basis).

Table 7 shows the results from the quantitative ^{13}C NMR analysis of two raw (non-treated) bio-oils and their respective upgraded oils using 100 g of γ-Al_2O_3 and HZSM-5/γ-Al_2O_3 at 500 °C. In addition, results from the ^{13}C NMR analysis of an FP oil obtained at an ablative FP unit at 530 °C are included for comparison. The ^{13}C NMR spectra are found in Fig. S7. The integration was performed following the procedure suggested by Ben and Ragauskas [61] and taking into account the modifications suggested by Happs et al. [52]. Comparing the two bio-oils collected without catalytic treatment at the LT-CFB and the FP oil obtained at lower pyrolysis temperature, it can be seen that with increasing pyrolysis temperature the contribution of carbonyls, aliphatic C–O, aliphatic C–H and methoxyl groups decreased, while the sum of aromatic C–C and C–H groups increased from 25% (530 °C) to 48% (660 °C).

The decreased oxygen content of the bio-oil (**Table 5**) and its decreased carbon yield towards increased pyrolysis temperature can be attributed partly to decarbonylation and decarboxylation. With increasing pyrolysis temperatures, the extent of cracking reactions of instable oxygenates such as aldehydes, ketones and acids lead to decarbonylation and decarboxylation , which results in the observed enhanced deoxygenation and lowered TAN yields towards higher pyrolysis temperatures. For acetol, an important pyrolysis vapor model compound, a conversion of 79% was reported in an empty stainless steel reactor at 650 °C under production of CO [8]. Steam reforming and dry reforming are highly endothermic reactions, and as such the extent of these reactions will increase at elevated temperatures, leading to the formation of hydrogen. In addition, the removal of methoxy-groups from lignin-derived methoxy-phenols will increase with temperature according to a radical mechanism, which increases the yields of phenols and CO. Due to the strong aryl-OH bond of phenolic compounds, the dissociation energy of this bond requires higher temperatures and activation energies, eventually leading to the formation of aromatics.

Upon catalytic treatment of the LT-CFB tars with HZSM-5/γ-Al_2O_3 at 500 °C, the contribution of aromatic C–C and C–H groups increased from 42% to 55%, while for γ-Al_2O_3 it increased only slightly from 48% to 50%. The increased aromatization activity of HZSM-5/γ-Al_2O_3 can be attributed to the confinement effect of the microporous HZSM-5 zeolite and Brønsted acid sites inside the channels. These observations agree with investigations using the ablative FP unit at lower temperatures of 530 °C and catalytically treating the vapors with HZSM-5, γ-Al_2O_3, and HZSM-5/γ-Al_2O_3 catalysts [41].

Table 7. Carbon percentage based on the ^{13}C NMR analysis of bio-oils collected at the LT-CFB gasifier for indicated pyrolysis chamber temperature and catalysts (100 g). Bio-oil collected for regular fast pyrolysis (FP) at 530 °C shown for reference.

Average pyrolysis chamber temperature [°C]	662		656		530 (FP)
Catalyst	-	γ-Al_2O_3, 500 °C	-	HZSM-5/γ-Al_2O_3, 500 °C	-
^{13}C NMR analysis					
Carbonyl (215–166.5 ppm)	7.2%	6.2%	9.4%	6.2%	14.6%
Aromatic C–O (166.5–142 ppm)	10.6%	7.9%	10.5%	8.3%	12.5%
Aromatic C–C (142–132/125 ppm)[a]	27.0%	8.5%	24.1%	9.2%	7.5%
Aromatic C–H (132/125–95.8 ppm)[a]	20.9%	41.0%	17.6%	45.7%	17.9%
Aliphatic C–O (95.8–60.8 ppm)	3.3%	2.4%	4.3%	2.3%	10.6%
Methoxyl (60.8–55.2)	0.6%	0.4%	1.0%	0.7%	5.0%
Aliphatic C–H (55.2–0 ppm, with exclusion of solvent)	30.4%	33.7%	33.1%	27.7%	31.8%

[a]For catalytically treated pyrolysis oils the border between aromatic C–C and aromatic C–H was moved downfield from 125 ppm to 132 ppm following the recommendation of Happs et al. [52].

Compared to 1D NMR spectra required for quantification, 2D NMR spectra lower the likelihood of overlapping because the signals are spread out into two dimensions. The heteronuclear single-quantum correlation spectroscopy (HSQC) correlates chemical shifts of carbons and protons in a phase sensitive way. The HSQC NMR spectra for the raw and upgraded tars using γ-Al_2O_3 and HZSM-5/γ-Al_2O_3 are provided in Fig. S8 and S9, respectively. The catalytic treatment with both catalysts clearly reduced the contributions of sugars (–CH–O–) and aldehydes. A higher contribution of the aromatic CH region resulted when using HZSM-5/γ-Al_2O_3 compared to γ-Al_2O_3, in agreement with 1D ^{13}C NMR analysis (**Table 7**).

The GC-MS/FID analysis of the phase separated aqueous and oil fraction is shown in **Fig. 8**. Besides the relative FID areas of different product groups (**Fig. 8** a+b), also the semi-quantitative yields are shown obtained by multiplication of the relative FID areas with the yield of water-free organics in each fraction. The aqueous fraction contained mainly alcohols, ketones, acids, and phenolics. Hydroxyacetone and levoglucosan were detected in the aqueous phase collected from the untreated producer gas, while those compounds were not detected after the catalytic treatment, indicating that these sugar derived compounds [62–65] were converted over the catalyst. The vapor treatment at a lower catalyst temperature of 450 °C with HZSM-5/γ-Al_2O_3 had the least effect on the compounds recovered in the aqueous phase (**Fig. 8** a), and as such did not markedly influence the yield of organics recovered in the aqueous phase. At a higher catalyst temperature of 500 °C, both γ-Al_2O_3 and HZSM-5/γ-Al_2O_3 decreased the concentration and the yield of acids recovered in the aqueous phase, while the increased concentration and yield of phenols in the aqueous phase is attributed to the cleavage of methoxy-groups from lignin derived methoxy-phenolics [62–64]. In the phase separated oil fraction, the yield of monoaromatics increased upon catalyst vapor treatment, especially for HZSM-5/γ-Al_2O_3 due to the shape selectivity of its micropore-structure. The highest concentrated monoaromatics are toluene, p-xylene, and benzene. The concentration of oxygenates in the oil phase decreased, in line with the vapor deoxygenation and the increased content of aromatics. The concentration of phenolics and small acids such as acetic, propanoic, and butanoic acid in the oil phase decreased by the catalytic treatment, which is in line with a reduced TAN (**Table 5**).

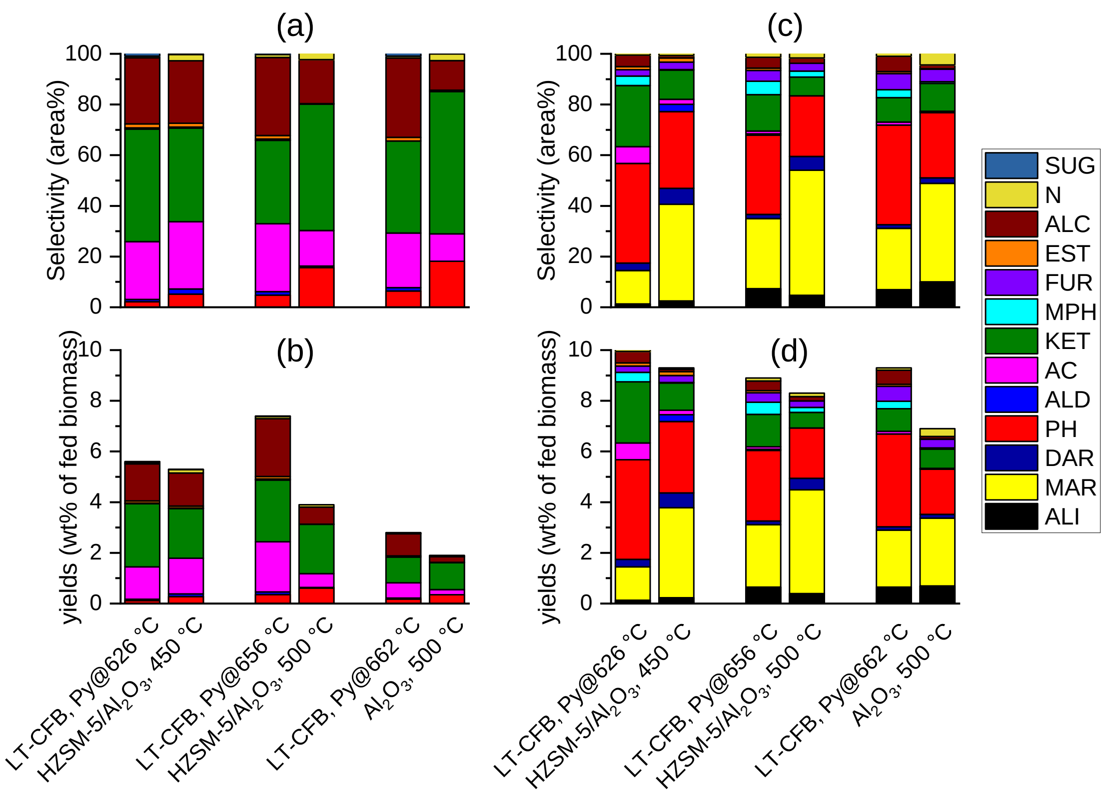

Fig. 8. GC-MS/FID analysis of aqueous and oil fraction. The products were grouped into aliphatics (ALI), monoaromatics (MAR), di-aromatics (DAR), phenols (PH), aldehydes (ALD), acids (AC), ketones (KET), methoxy-phenols (MPH), furans (FUR), esters (EST), alcohols (ALC), nitrogen containing compounds (N), and (anhydro-)sugars. **(**a) Selectivity of compounds (grouped) in aqueous phase. (b) Semi-quantitative yields of product groups in aqueous phase. (c) Selectivity of compounds (grouped) in oil phase. (d) Semi-quantitative yields of product groups in oil phase.

Basic nitrogen is a well-known catalyst poison in catalytic cracking [66–68]. For conventional refinery feedstock, the content of basic nitrogen is usually about one third of the total nitrogen [68–70]. Basic nitrogen compounds may reduce the cracking activity by (i) site competition due to their reversible adsorption to Brønsted and Lewis acid sites, and (ii) acting as coke precursors due to their size and aromatic nature. As we showed recently [56], a poor cracking performance resulted when co-feeding pyrolysis oils derived from wheat straw with vacuum gas oil to a microactivity test unit. This was partly attributed to the elevated basic nitrogen content of wheat straw oils (0.43- 0.55 mass-% basic nitrogen), while blending with wood derived oil (0.03 mass-% basic nitrogen) did not markedly influence the cracking performance. The tars collected in this work from the gasification of wheat straw in the LT-CFB gasifier showed a higher content of basic nitrogen compared to oil obtained at a FP temperature of 530 °C (Fig. 9). This can be attributed to the elevated temperatures of the gasifier as a positive correlation between basic nitrogen content of collected oils and temperature of the LT-CFB pyrolysis chamber was found (see Fig. 9). The up to four times higher basic nitrogen content of the bio-oils collected at the LT-CFB would likely impede the utilization of the bio-oil as a feedstock for catalytic cracking due to poisoning of the FCC catalyst without initial decrease in basic nitrogen by e.g. hydrotreating. The corrosiveness of the collected bio-oils can be expected to decrease for oils collected at higher pyrolysis temperature according to the negative correlation observed between TAN and pyrolysis temperature (Fig. 9).

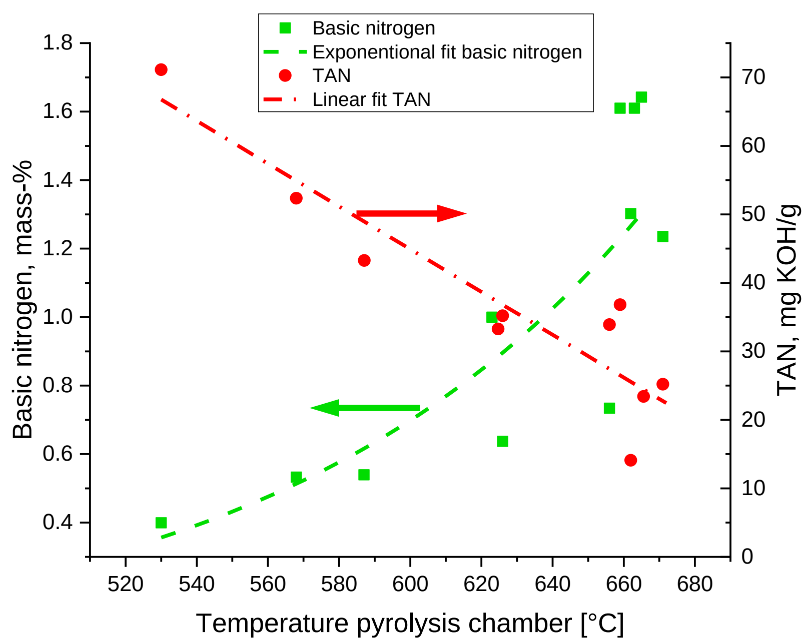

Fig. 9. Basic nitrogen content and TAN of tars collected at different pyrolysis temperatures. Note that the data points at 530 °C were obtained from oil produced using an ablative fast pyrolysis unit while all other data points were obtained using the LT-CFB gasifier.

3.5 Coke

The results of the quantification of coke on the catalysts by combustion and integration of the combustion products CO and CO_2 are summarized in **Table 8**. The higher coke loading of 30 g HZSM-5/γ-Al_2O_3 as opposed to 100 g can be explained by the longer tar sampling period and higher WHSV, and thus a higher tar load. 100 g γ-Al_2O_3 showed a higher coking propensity compared to zeolite containing HZSM-5/γ-Al_2O_3, which is in agreement with our recent work [41].

Table 8. Overview of coke loadings in terms of wt% carbon per coke-free catalyst.

	coke wt% C per coke-free catalyst
30 g HZSM-5/γ-Al_2O_3, 500 °C	15.7%
100 g HZSM-5/γ-Al_2O_3, 500 °C	14.1%
100 g HZSM-5/γ-Al_2O_3, 450 °C	10.4%
100 g γ-Al_2O_3, 500 °C	19.4%

We further investigated the combustion profile and found that coke on γ-Al_2O_3 combusted at lower temperatures compared to HZSM-5/γ-Al_2O_3 (**Fig. 10**), in agreement with literature [41,47,71]. The coking at a catalyst temperature of 500 °C was studied for the same biomass but at lower FP temperature of 530 °C using a tandem micropyrolyzer system, described in more detail in ref. [56], for an ex-situ located catalyst (2 mg) and a cumulative biomass-to-catalyst ratio of ~4. Despite the difference in scale and lower pyrolysis temperature used at the micro-pyrolyzer, similar combustion profiles resulted (**Fig. 10**).

As such, it appears that the coke species do not differ much with variation in pyrolysis temperature. However, the reduced tar yield at the higher operating temperature of the LT-CFB gasifier reduces the tar load on the catalyst and therefore longer runtimes can be expected until the quality of the bio-oil deteriorates and catalyst regeneration is required. For continuous operation, a parallel fixed bed scenario or a circulating fluidized bed is required in order to operate the regeneration of the catalyst simultaneously to the catalytic upgrading [72,73].

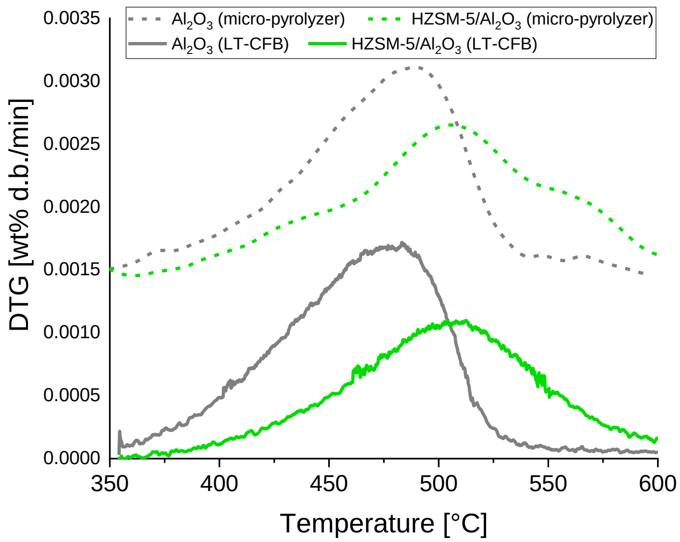

Fig. 10. Coke combustion profiles from coked catalyst obtained from the LT-CFB at a FP temperature of ~660 °C and using a tandem micro-pyrolyzer [74] with a FP temperature of 530 °C. The catalyst temperature was 500 °C in both systems. For clarity, the micro-pyrolyzer curves were shifted upwards by 0.0015.

3.6 Limitations and future development

It is known from studies of fast pyrolysis of biomass that the optimum bio-oil yield is obtained at ~500–550 °C [49–54]. As such, the temperatures obtained in this study is above the maximum as is clearly seen from the level of tar in the producer gas. Some further decrease in pyrolysis temperature below the ~570 °C could probably be achieved by further decreasing the particle circulation rate, but the temperature decrease will increase the char yield and reduce the flow of sensible heat (thermal enthalpy) exiting the gasifier with the raw product gas. The latter means that less air (or O_2) can be added (at a fixed char reactor temperature and limited water addition), which will also lead to a higher char concentration in the bed particles. This may negatively affect the function of the L-leg (returning particles from the primary cyclone to the char reactor). On the other hand, the bio-oil obtained in this study is already partly de-oxygenated compared to bio-oil obtained at the temperature of maximum yield, which may be considered as an advantage.

With respect to the flexibility of the proposed polygeneration scheme: If the wind is blowing and the sun is shining, there is no additional demand for heat and electricity production by gasification of biomass and therefore the temperature of the LT-CFB pyrolysis chamber can be lowered in order to increase the tar yields and store energy as bio-oil. As the TAN of the tars increases with decreasing pyrolysis temperature and the tar loading on the catalyst increases, the catalyst will need to be regenerated more frequently in order to prevent a deterioration in fuel properties. In this regard, it is beneficial that the basic nitrogen content decreases with decreasing temperature. While the tars collected at higher pyrolysis temperature already show a reduced TAN, the catalytic treatment helped in reducing the basic nitrogen content, but it could be considered to collect the tars generated at higher pyrolysis temperatures without catalytic treatment and subject them directly to hydro-cracking/treatment. In any case, an efficient tar collection system is required in order to valorize the tars for fuel purpose and protect downstream gas engines from tar deposition.

Possibilities for future development of the system include:

- Testing of catalytic bed material that can tolerate high temperatures in the gasification reactor and which does not loose catalytic activity by the direct contact with the biomass and the hydrothermal conditions.
- For downstream catalytic production of chemicals/fuels from the dry gasses remaining after tar condensation, decreasing the amount of introduced nitrogen by replacing the air inlet stream with a mixture of O_2/CO_2 or O_2/steam will provide a better syngas quality. For combustion of the gases in an engine, the dilution with N_2 is of lower importance.

- Future development could also include the testing of hydrodeoxygenation catalysts, which use hydrogen to selectively remove oxygen as water without breaking the C-C bonds. This may have the potential to incorporate some of the hydrogen that is present in the producer gas in the bio-oil and thereby obtain higher energy recoveries of bio-oil may be obtained.

4 CONCLUSION

The processing of wheat straw in an LT-CFB gasifier aimed at producing bio-oil, producer gas for combustion in an engine to produce electricity and heat, and char for soil improvement rather than aiming at maximizing a single product. The concept is thus novel compared to previous concepts typically aiming at maximizing bio-oil or syn-gas.

Increased operating temperature of the pyrolysis chamber of the gasifier reduced the bio-oil yield but increased its quality, such as increased heating value and decreased moisture content, oxygen content, and TAN.

Parallel sampling of tars with and without catalytic treatment was used in order to investigate the effect of the catalytic treatment on the bio-oil quality. The in-line catalytic treatment of tars using HZSM-5/γ-Al_2O_3 or γ-Al_2O_3 as catalysts significantly improved the quality of the collected bio-oils since the moisture content, oxygen content, TAN and basic nitrogen content decreased while the heating value of the oils was improved. . For a similar improvement in oxygen content and TAN of the bio-oils from ~13-14 wt% O and 14-34 mg KOH/g TAN to 10-11 wt% O and 3-5 mg KOH/g TAN, the energy recovery of the bio-oil decreased by only ~2 percentage points when using HZSM-5/γ-Al_2O_3 as catalyst while it decreased by ~4 percentage points when γ-Al_2O_3 was used as catalyst. The catalytically treated bio-oils showed a decreased charring propensity and are expected to be better suited for further processing in existing oil refineries.

ASSOCIATED CONTENT

Supporting Information

Wheat straw analysis by sulfuric acid hydrolysis; Content of carbohydrates and Klason lignin in feedstock; Temperature of catalyst during in-line treatment of LT-CFB producer gas; Mass balance data; Argon high-resolution low temperature isotherms; ^{1}H NMR spectra of coked catalysts; thermogravimetric analysis of bio-oils during heating; ^{13}C NMR spectra of bio-oils; 2D HSQC NMR spectra of bio-oils;

AUTHOR INFORMATION

Corresponding Author:

* aj@kt.dtu.dk (Anker Degn Jensen)

Author Contributions

The manuscript was written through contributions of all authors. All authors have given approval to the final version of the manuscript.

Funding Sources

Funding by the Danish Energy Technology Development and Demonstration Program (EUDP project number 12454) is gratefully acknowledged.

ACKNOWLEDGMENT

The sulfuric acid hydrolysis of the biomass feedstock was conducted by Dr. Zsuzsa Sárossy and her help is gratefully acknowledged. The NMR data were recorded at the NMR Center at DTU supported by the Villum Foundation. The help of Peder Stoholm (Danish Fluid Bed Technology) with operating the gasifier is gratefully acknowledged.

ABBREVIATIONS

CFP, catalytic fast pyrolysis; daf, dry and ash-free; FP, fast pyrolysis; LT-CFB, low temperature circulating fluidized bed; TGA, thermogravimetric analysis; TPD, temperature-programmed desorption;

REFERENCES

[1] Sigurjonsson HÆ, Elmegaard B, Clausen LR, Ahrenfeldt J. Climate effect of an integrated wheat production and bioenergy system with Low Temperature Circulating Fluidized Bed gasifier. Appl Energy 2015;160:511–20. https://doi.org/10.1016/j.apenergy.2015.08.114.

[2] Jensen PA, Frandsen FJ, Dam-Johansen K, Sander B. Experimental Investigation of the Transformation and Release to Gas Phase of Potassium and Chlorine during Straw Pyrolysis. Energy and Fuels 2000;14:1280–5. https://doi.org/10.1021/ef000104v.

[3] Ahrenfeldt J, Thomsen TP, Henriksen U, Clausen LR. Biomass gasification cogeneration - A review of state of the art technology and near future perspectives. Appl Therm Eng 2013;50:1407–17. https://doi.org/10.1016/j.applthermaleng.2011.12.040.

[4] Nielsen RG. Optimering af Lav Temperatur Cirkulerende Fluid Bed forgasningsprocessen til biomasse med højt askeindhold. Technical University of Denmark, 2007.

[5] DONG Energy Power A/S, Danish Fluid Bed Technology (DFBT), Technical Univeristy of Denmark. B4C – Biomass for Conversion; Pyroneer Gasification Technology Development. 2015.

[6] Stoholm P, J C, Nielsen RG, B. S, J. A, Henriksen U.B. The low temperature CFB gasifier—100 kWth tests on straw and new 6 MWth demonstration plant. Proc. 18th Eur. biomass Conf. 2010, Lyon, Lyon: n.d., p. 619–23.

[7] DONG Energy A/S. GASOLUTION – Enables efficient power and gas production. 2015.

[8] Thomsen TP, Ravenni G, Holm JK, Ahrenfeldt J, Hauggaard-Nielsen H, Henriksen UB. Screening of various low-grade biomass materials for low temperature gasification: Method development and application. Biomass and Bioenergy 2014;79:128–44. https://doi.org/10.1016/j.biombioe.2014.12.019.

[9] Thomsen TP, Sárossy Z, Gøbel B, Stoholm P, Ahrenfeldt J, Frandsen FJ, et al. Low temperature circulating fluidized bed gasification and co-gasification of municipal sewage sludge. Part 1: Process performance and gas product characterization. Waste Manag 2017;66:123–33. https://doi.org/10.1016/j.wasman.2017.04.028.

[10] Bruun EW, Petersen CT, Hansen E, Holm JK, Hauggaard-Nielsen H. Biochar amendment to coarse sandy subsoil improves root growth and increases water retention. Soil Use Manag 2014;30:109–18. https://doi.org/10.1111/sum.12102.

[11] Hansen V, Müller-Stöver D, Ahrenfeldt J, Holm JK, Henriksen UB, Hauggaard-Nielsen H. Gasification biochar as a valuable by-product for carbon sequestration and soil amendment. Biomass and Bioenergy 2015;72:300–8. https://doi.org/10.1016/j.biombioe.2014.10.013.

[12] Thomsen TP, Hauggaard-Nielsen H, Gøbel B, Stoholm P, Ahrenfeldt J, Henriksen UB, et al. Low temperature circulating fluidized bed gasification and co-gasification of municipal sewage sludge. Part 2: Evaluation of ash materials as phosphorus fertilizer. Waste Manag 2017;66:145–54. https://doi.org/10.1016/j.wasman.2017.04.043.

[13] Zwart R, Heijden S Van Der, Emmen R, Bentzen JD, Stoholm P, Krogh J. Tar removal from low-temperature gasifiers. 2010.

[14] Czernik S, Bridgwater A V. Overview of applications of biomass fast pyrolysis oil. Energy & Fuels 2004;18:590–598. https://doi.org/10.1021/ef034067u.

[15] Oasmaa A, Czernik S. Fuel oil quality of biomass pyrolysis oil - State of the art for the end users. Energy & Fuels 1999;13:914–21. https://doi.org/10.1021/ef980272b.

[16] Fjellerup J, Gøbel B, Ahrenfeldt J, Henriksen U. Formation , Decomposition and Cracking of Biomass Tars in Gasification. 2005. https://doi.org/87-7475-326-6.

[17] Sundac N. Catalytic cracking of tar from biomass gasification 2007:1–6. https://doi.org/10.1007/s13399-012-0063-1.

[18] Shen Y, Yoshikawa K. Recent progresses in catalytic tar elimination during biomass gasification or pyrolysis - A review. Renew Sustain Energy Rev 2013;21:371–92. https://doi.org/10.1016/j.rser.2012.12.062.

[19] Devi L, Ptasinski KJ, Janssen FJJG, Van Paasen SVB, Bergman PCA, Kiel JHA. Catalytic decomposition of biomass tars: Use of dolomite and untreated olivine. Renew Energy 2005;30:565–87. https://doi.org/10.1016/j.renene.2004.07.014.

[20] Guan G, Kaewpanha M, Hao X, Wang Z, Cheng Y, Kasai Y, et al. Promoting effect of potassium addition to calcined scallop shell supported catalysts for the decomposition of tar derived from different biomass resources. Fuel 2013;109:241–7. https://doi.org/10.1016/j.fuel.2012.11.074.

[21] Asadieraghi M, Mohd W, Wan Daud WMA, Abbas HF. Heterogeneous catalysts for advanced bio-fuel production through catalytic biomass pyrolysis vapor upgrading : a review. RSC Adv 2015;5:22234–55. https://doi.org/10.1039/C5RA00762C.

[22] Saraeian A, Nolte MW, Shanks BH. Deoxygenation of biomass pyrolysis vapors: Improving clarity on the fate of carbon. Renew Sustain Energy Rev 2019;104:262–80. https://doi.org/10.1016/j.rser.2019.01.037.

[23] Carlson TR, Tompsett GA, Conner WC, Huber GW. Aromatic production from catalytic fast pyrolysis of biomass-derived feedstocks. Top Catal 2009;52:241–52. https://doi.org/10.1007/s11244-008-9160-6.

[24] Jae J. Production of green aromatics and olefins from lignocellulosic biomass by catalytic fast pyrolysis: Chemistry, catalysis, and process development. Chem Eng 2012;PhD.

[25] Hernando H, Fermoso J, Ochoa-Hernández C, Opanasenko M, Pizarro P, Coronado JM, et al. Performance of MCM-22 zeolite for the catalytic fast-pyrolysis of acid-washed wheat straw. Catal Today 2017. https://doi.org/10.1016/j.cattod.2017.09.043.

[26] Aho A, Kumar N, Eränen K, Salmi T, Hupa M, Murzin DY. Catalytic Pyrolysis of Biomass in a Fluidized Bed Reactor: Influence of the Acidity of H-Beta Zeolite. Process Saf Environ

Prot 2007;85:473–80. https://doi.org/10.1205/psep07012.

[27] Fermoso J, Hernando H, Jana P, Moreno I, Prech J, Ochoa-Herndndez C, et al. Lamellar and pillared ZSM-5 zeolites modified with MgO and ZnO for catalytic fast-pyrolysis of eucalyptus woodchips. Catal Today 2016;277:171–81. https://doi.org/10.1016/j.cattod.2015.12.009.

[28] Kim P, Rials TG, Labbé N, Chmely SC. Screening of Mixed-Metal Oxide Species for Catalytic Ex Situ Vapor-Phase Deoxygenation of Cellulose by py-GC/MS Coupled with Multivariate Analysis. Energy and Fuels 2016;30:3167–74. https://doi.org/10.1021/acs.energyfuels.6b00347.

[29] Kalogiannis KG, Stefanidis SD, Karakoulia SA, Triantafyllidis KS, Yiannoulakis H, Michailof C, et al. First pilot scale study of basic vs acidic catalysts in biomass pyrolysis: Deoxygenation mechanisms and catalyst deactivation. Appl Catal B Environ 2018;238:346–57. https://doi.org/10.1016/j.apcatb.2018.07.016.

[30] Galadima A, Muraza O. In situ fast pyrolysis of biomass with zeolite catalysts for bioaromatics/gasoline production: A review. Energy Convers Manag 2015;105:338–54. https://doi.org/10.1016/j.enconman.2015.07.078.

[31] Wan S, Wang Y. A review on ex situ catalytic fast pyrolysis of biomass. Front Chem Sci Eng 2014;8:280–94. https://doi.org/10.1007/s11705-014-1436-8.

[32] Liu C, Wang H, Karim AM, Sun J, Wang Y. Catalytic fast pyrolysis of lignocellulosic biomass. Chem Soc Rev 2014;43:7594–623. https://doi.org/10.1039/C3CS60414D.

[33] Lappas AA, Samolada MC, Iatridis D, Voutetakis S, Vasalos IA. Biomass pyrolysis in a circulating fluid bed reactor for the production of fuels and chemicals. Fuel 2002;81:2087–2095.

[34] Paasikallio V, Lindfors C, Kuoppala E, Solantausta Y, Oasmaa A, Lehto J, et al. Product quality and catalyst deactivation in a four day catalytic fast pyrolysis production run. Green Chem 2014;16:3549–59. https://doi.org/10.1039/c4gc00571f.

[35] Mante OD, Dayton DC, Carpenter JR, Wang K, Peters JE. Pilot-scale catalytic fast pyrolysis of loblolly pine over y-Al2O3 catalyst. Fuel 2018;214:569–79. https://doi.org/10.1016/j.fuel.2017.11.073.

[36] Mazanec TJ, Whiting JP, Pesa F, Song R, Cheng Y-T, Song R. Regeneration of catalytic fast pyrolysis. US 2014/0303414 A1, 2017.

[37] Shi J, Sorensen C, Mazanec T, Song R, Goud S, Han S, et al. Improved catalytic fast pyrolysis process with impurity removal. WO2017003790A1, 2015.

[38] Kalogiannis KG, Stefanidis SD, Lappas AA. Catalyst deactivation, ash accumulation and bio-oil deoxygenation during ex situ catalytic fast pyrolysis of biomass in a cascade thermal-catalytic reactor system. Fuel Process Technol 2019;186:99–109. https://doi.org/10.1016/j.fuproc.2018.12.008.

[39] Eschenbacher A, Jensen PA, Henriksen UB, Ahrenfeldt J, Li C, Duus JØ, et al. Impact of ZSM-5 deactivation on bio-oil quality during upgrading of straw derived pyrolysis vapors. Energy & Fuels 2019;33:397–412. https://doi.org/10.1021/acs.energyfuels.8b03691.

[40] Eschenbacher A, Jensen PA, Henriksen UB, Ahrenfeldt J, Ndoni S, Li C, et al. Catalytic deoxygenation of vapors obtained from ablative fast pyrolysis of wheat straw using mesoporous HZSM-5. Fuel Process Technol 2019;194:106119. https://doi.org/10.1016/J.FUPROC.2019.106119.

[41] Eschenbacher A, Jensen PA, Henriksen UB, Ahrenfeldt J, Li C, Duus JØ, et al. Deoxygenation of wheat straw fast pyrolysis vapors using HZSM-5, Al2O3 , HZSM-5/Al2O3 extrudates, and desilicated HZSM-5/Al2O3 extrudates. Energy & Fuels 2019:acs.energyfuels.9b00906. https://doi.org/10.1021/acs.energyfuels.9b00906.

[42] Stefanidis SD, Kalogiannis KG, Iliopoulou EF, Lappas AA, Pilavachi PA. In-situ upgrading of biomass pyrolysis vapors: Catalyst screening on a fixed bed reactor. Bioresour Technol 2011;102:8261–7. https://doi.org/10.1016/j.biortech.2011.06.032.

[43] Yorgun S, Şimşek YE. Catalytic pyrolysis of Miscanthus × giganteus over activated alumina. Bioresour Technol 2008;99:8095–100. https://doi.org/10.1016/j.biortech.2008.03.036.

[44] Ateş F, Işikdağ MA. Influence of temperature and alumina catalyst on pyrolysis of corncob. Fuel 2009;88:1991–7. https://doi.org/10.1016/j.fuel.2009.03.008.

[45] Demiral I, Şensöz S. The effects of different catalysts on the pyrolysis of industrial wastes (olive and hazelnut bagasse). Bioresour Technol 2008;99:8002–7. https://doi.org/10.1016/j.biortech.2008.03.053.

[46] Samolada MC, Papafotica A, Vasalos IA. Catalyst Evaluation for Catalytic Biomass Pyrolysis. Energy & Fuels 2000;14:1161–7. https://doi.org/10.1021/ef000026b.

[47] Du S, Gamliel DP, Valla JA, Bollas GM. The effect of ZSM-5 catalyst support in catalytic pyrolysis of biomass and compounds abundant in pyrolysis bio-oils. J Anal Appl Pyrolysis 2016;122:7–12. https://doi.org/10.1016/j.jaap.2016.11.002.

[48] Baldwin RM, Feik CJ. Bio-oil stabilization and upgrading by hot gas filtration. Energy and Fuels 2013;27:3224–38. https://doi.org/10.1021/ef400177t.

[49] Akhtar J, Saidina Amin N. A review on operating parameters for optimum liquid oil yield in biomass pyrolysis. Renew Sustain Energy Rev 2012;16:5101–9. https://doi.org/10.1016/j.rser.2012.05.033.

[50] Channiwala SA, Parikh PP. A unified correlation for estimating HHV of solid, liquid and gaseous fuels. Fuel 2002;81:1051–63. https://doi.org/10.1016/S0016-2361(01)00131-4.

[51] Schofield K. The enigmatic mechanism of the flame ionization detector: Its overlooked implications for fossil fuel combustion modeling. Prog Energy Combust Sci 2008;34:330–50. https://doi.org/10.1016/j.pecs.2007.08.001.

[52] Happs RM, Iisa K, Iii JRF. Quantitative 13C NMR characterization of fast pyrolysis oils. RSC Adv 2016;6:102665–70. https://doi.org/10.1039/C6RA24044E.

[53] Stoholm P, Nielsen RG, Nygaard H, Tobiasen L, Fock MW, Richardt K, et al. Low temperature CFB gasifier conceptual ideas, applications and first test results. Biomass Energy Ind 2000.

[54] Nielsen RG, Stoholm P, Nielsen MB, Krogh J, Nørholm N, Antonsen S, et al. the Lt-Cfb

Gasifier - First Test Results From the 500 Kw Test Plant. 14th Eur Biomass Conf 2005.

[55] Jensen CD, Ahrenfeldt J. Characterization of product gas from gasification of straw in an LT-CFB gasifier, for the catalytic conversion of tar to bio-oil. Technical University of Denmark, 2018.

[56] Eschenbacher A, Myrstad T, Bech N, Duus JØ, Li C, Jensen PA, et al. Co-processing of wood and wheat straw derived pyrolysis oils with FCC feed — Product distribution and effect of deoxygenation. Fuel 2020;260:116312. https://doi.org/10.1016/j.fuel.2019.116312.

[57] Starace AK, Black BA, Lee DD, Palmiotti EC, Orton KA, Michener WE, et al. Characterization and Catalytic Upgrading of Aqueous Stream Carbon from Catalytic Fast Pyrolysis of Biomass. ACS Sustain Chem Eng 2017:acssuschemeng.7b03344. https://doi.org/10.1021/acssuschemeng.7b03344.

[58] Hall PH. Recovering valuable products from the aqueous streams of fast pyrolysis. Iowa State University, 2017.

[59] Mukarakate C, Evans RJ, Deutch S, Evans T, Starace AK, Ten Dam J, et al. Reforming Biomass Derived Pyrolysis Bio-oil Aqueous Phase to Fuels. Energy and Fuels 2017;31. https://doi.org/10.1021/acs.energyfuels.6b02463.

[60] Gayubo AG, Aguayo AT, Atutxa A, Prieto RR, Bilbao J, Aguayo T. Deactivation of a HZSM-5 Zeolite Catalyst in the Transformation of the Aqueous Fraction of Biomass Pyrolysis Oil into Hydrocarbons. Energy and Fuels 2004;18:1640–7. https://doi.org/10.1021/ef040027u.

[61] Ben H, Ragauskas AJ. Heteronuclear single-quantum correlation-nuclear magnetic resonance (HSQC-NMR) fingerprint analysis of pyrolysis oils. Energy and Fuels 2011;25:5791–801. https://doi.org/10.1021/ef201376w.

[62] Negahdar L, Gonzalez-Quiroga A, Otyuskaya D, Toraman HE, Liu L, Jastrzebski JTBH, et al. Characterization and Comparison of Fast Pyrolysis Bio-oils from Pinewood, Rapeseed Cake, and Wheat Straw Using13C NMR and Comprehensive GC × GC. ACS Sustain Chem Eng 2016;4:4974–85. https://doi.org/10.1021/acssuschemeng.6b01329.

[63] Ates F, Tophanecioglu S, Putun AE. The evaluation of mesoporous materials as catalyst in fast pyrolysis of wheat straw. Int J Green Energy 2015;12:57–64. https://doi.org/10.1080/15435075.2014.889005.

[64] Yang Q, Wu S. Wheat straw pyrolysis analysis by thermogravimetry and gas chromatography-mass spectrometry. Cellul Chem Technol 2009;43:123–31.

[65] Patwardhan PR, Dalluge DL, Shanks BH, Brown RC. Distinguishing primary and secondary reactions of cellulose pyrolysis. Bioresour Technol 2011;102:5265–9. https://doi.org/10.1016/j.biortech.2011.02.018.

[66] Mills GA, Boedeker ER, Oblad AG. Chemical Characterization of Catalysts. I. Poisoning of Cracking Catalysts by Nitrogen Compounds and Potassium Ion. J Am Chem Soc 1950;72:1554–60. https://doi.org/10.1021/ja01160a035.

[67] Caeiro G, Costa AF, Cerqueira HS, Magnoux P, Lopes JM, Matias P, et al. Nitrogen poisoning effect on the catalytic cracking of gasoil. Appl Catal A Gen 2007;320:8–15.

https://doi.org/10.1016/j.apcata.2006.11.031.

[68] Sheng Q, Wang G, Liu Y, Husein MM, Gao C, Gao J. Pilot-scale evaluation of hydrotreating inferior coker gas oil prior to its fluid catalytic cracking. Fuel 2018;226:27–34. https://doi.org/10.1016/j.fuel.2018.03.150.

[69] Fu CM, Schaffer AM. Effect of Nitrogen Compounds on Cracking Catalysts. Ind Eng Chem Prod Res Dev 1985;24:68–75. https://doi.org/10.1021/i300017a013.

[70] Chen X, Liu Y, Li S, Feng X, Shan H, Yang C. Structure and Composition Changes of Nitrogen Compounds during the Catalytic Cracking Process and Their Deactivating Effect on Catalysts. Energy and Fuels 2017;31:3659–68. https://doi.org/10.1021/acs.energyfuels.6b03230.

[71] Du S, Sun Y, Gamliel DP, Valla JA, Bollas GM. Catalytic pyrolysis of miscanthus×giganteus in a spouted bed reactor. Bioresour Technol 2014;169:188–97. https://doi.org/10.1016/j.biortech.2014.06.104.

[72] Dutta A, Schaidle JA, Humbird D, Baddour FG, Sahir A. Conceptual Process Design and Techno-Economic Assessment of Ex Situ Catalytic Fast Pyrolysis of Biomass: A Fixed Bed Reactor Implementation Scenario for Future Feasibility. Top Catal 2016;59:2–18. https://doi.org/10.1007/s11244-015-0500-z.

[73] Griffin MB, Iisa K, Wang H, Dutta A, Orton KA, French RJ, et al. Driving towards cost-competitive biofuels through catalytic fast pyrolysis by rethinking catalyst selection and reactor configuration. Energy Environ Sci 2018;11:2904–18. https://doi.org/10.1039/c8ee01872c.

[74] Eschenbacher A, Goodarzi F, Saraeian A, Kegnæs S, Shanks BH, Jensen AD. Performance of Mesoporous HZSM-5 and Silicalite-1 Coated Mesoporous HZSM-5 Catalysts for Deoxygenation of Straw Fast Pyrolysis Vapors. J Anal Appl Pyrolysis 2019:104712. https://doi.org/10.1016/J.JAAP.2019.104712.